

Intra-event evolution of elemental and ionic concentrations in wet deposition in an urban environment

Thomas Audoux¹, Benoit Laurent¹, Karine Desboeufs¹, Gael Noyalet¹, Franck Maisonneuve², Olivier Laurent^{2,3}, Servanne Chevaillier²

¹ Université Paris Cité and Univ Paris Est Creteil, CNRS, LISA, F-75013, Paris, France

² Univ Paris Est Creteil and Université Paris Cité, CNRS, LISA, F-94010, Créteil, France

³ Univ Paris Est Creteil, CNRS, ENPC, Université Paris Cité, OSU-EFLUVE, F-94010, Créteil, France

Correspondence to: Thomas Audoux (thomas.audoux@lisa.ipsl.fr) ; Benoit Laurent (benoit.laurent@lisa.ipsl.fr)

Abstract.

~~Wet deposition is a crucial process that affects the lifetime of atmospheric particles by allowing them to be deposited by two different mechanisms, namely below the cloud and in the cloud. In order to estimate the mechanisms implied in the wet deposition, a measurement campaign was carried out~~conducted in the Paris region ~~to monitor, focusing on~~ the evolution of ~~the~~ chemical composition of wet deposition during rainfall events ~~from sequential sampling. A total of eight rain events have been sampled. The latter had different~~were documented and ~~characterized by varying~~ meteorological conditions, atmospheric dynamics, and aerosol ~~particulates~~particle concentrations. ~~Concomitant measurements representative of the chemical composition of aerosol particles~~urban conditions and ~~wet deposition allows calculating washout ratios from measurements taken at the beginning of the rainfall events, before the dilution effect occurred, and showed an increasing trend with increasing rainfall rates~~influenced by long-range mineral dust transport. The intra-event evolution of the chemical composition of wet deposition revealed the predominant role of meteorological parameters and local sources in the observed mass concentration variability. ~~The contributions of in-cloud and below cloud scavenging mechanisms were estimated for some rainfall events and found to vary depending on the specific sources, atmospheric dynamics and meteorological conditions.~~From selected case studies, the washout ratios (WR) and scavenging coefficients were ~~quantified by conducting simultaneous measurements of aerosol particle composition and wet deposition. The results highlighted a variability of the WR and scavenging coefficients depending on the rainfall rate and on the chemical specie. Scavenging coefficients estimated from WR ranged from 5.4×10^{-8} to $1.1 \times 10^{-5} \text{ s}^{-1}$ for chemical elements, and are within the range of values reported in the literature for $0.2\text{-}2 \mu\text{m}$ particles diameter. Our results pointed out that scavenging coefficient increases with rainfall rate according to a power law, as previously shown in the literature, indicating a stronger removal of particles from the atmosphere with greater precipitation intensity. Quantitative analysis of the data allowed us to estimate the relative contributions of in-cloud scavenging (ICS) for selected rain events. The ICS relative contributions ranged on average from 23% to 62% depending on the rain events, and varied according to the chemical species within the same rain event. This highlights the variability and complexity of the wet deposition process and the influence of specific factors on the contribution of ICS, such as aerosol particle size and hygroscopicity.~~ Overall, this study highlights the variability of wet deposition and its chemical composition, and the need to consider the specificities of each event to fully understand the underlying mechanisms.

38 1 Introduction

39 ~~After emissions or formations and transport of aerosols in the atmosphere, wet deposition is one of the final sinks~~
40 ~~in their atmospheric cycle (e.g.,~~ Wet deposition involves two distinct mechanisms: in-cloud scavenging (hereafter
41 referred to as ICS) and below cloud scavenging (hereafter referred to as BCS). ICS refers to the scavenging of
42 aerosols within the cloud, where they either act as condensation (or ice) nuclei or are captured by already formed
43 droplets (Seinfeld and Pandis, 2016). BCS is the result of particles being captured through collision by raindrops
44 as they fall ~~via several size-related mechanisms (e.g., Brownian diffusion, interception, inertial impaction;~~ (Slinn,
45 1977). Through these two mechanisms, wet deposition includes locally emitted aerosols that can be scavenged
46 from the atmosphere, as well as long-range transported aerosols that can be removed by precipitating cloud systems
47 (e.g., Bertrand et al., 2008). ~~Depending on the regions, wet deposition mechanisms collect atmospheric aerosols~~
48 ~~from different (natural, anthropogenic) sources that can be identified by their chemical composition. By~~
49 ~~scavenging atmospheric pollutants and potentially toxic metals, wet deposition has an impact on air quality. Wet~~
50 ~~deposition of nitrogen (N), phosphorus (P) and trace metals can also serve as a significant input of nutrients species~~
51 ~~to terrestrial and marine ecosystems (e.g.,~~

52 ~~Worldwide observational measurement networks have shown strong spatial and temporal variability in the mass~~
53 ~~and chemical flux of wet deposition. This variability can be observed at interannual, seasonal, daily, or intra-event~~
54 ~~scales and is dependent on the aerosol content, precipitation properties, and their interaction. Approaches based~~
55 ~~on only some of the measurable parameters have been used to document the scavenging of atmospheric particles~~
56 ~~by precipitation. One approach is to compute the washout ratio (hereafter referred to as WR), which is based on~~
57 ~~the ratio of the mass or elemental concentrations of wet deposition to those of aerosols measured in the atmosphere~~
58 ~~. WR is a parameter that integrates, without distinction of processes, the relative scavenging efficiency of~~
59 ~~particulate compounds and chemical elements by considering their transfer from air to water. WR has been~~
60 ~~regularly used to characterize wet deposition by precipitation for different types of particulate aerosols and~~
61 ~~chemical compounds found in various atmospheric environments.~~

62 The proportion of ICS and BCS in wet deposition is influenced by a number of factors, including the local
63 environment (e.g., rural, or urban) and associated emissions, meteorological variables such as rainfall amount,
64 intensity and type, and aerosols content in the atmosphere such as its loading, their size and vertical distributions
65 (Aikawa et al., 2014; Ge et al., 2016; Lim et al., 1991; Bertrand et al., 2008; Ge et al., 2021a). The accuracy of the
66 representation of these mechanisms in global and regional modeling is still questionable (Croft et al., 2010), as
67 there is insufficient data to constrain them accurately (Ryu and Min, 2022). Indeed, ~~while~~ BCS was considered to
68 be less important than ICS regarding wet deposition in several modeling studies (Croft et al., 2010; Yang et al.,
69 2015; Kim et al., 2021). ~~However,~~ recent ~~observational~~ observation studies have found that BCS ~~represented~~ could
70 represent a ~~non-negligible~~ significant fraction of the wet deposition (Xu et al., 2019; Ge et al., 2021a; Chatterjee et
71 al., 2010; Karşı et al., 2018; Audoux et al., 2023). Grythe et al. (2017) also emphasized the significance of BCS,
72 indicating that it is more responsible for the removal of aerosols in the lower atmosphere, while ICS dominates the
73 wet removal in the free troposphere. These recent findings demonstrate the need to re-evaluate the importance of
74 BCS in regional and global-scale modeling of atmospheric aerosols and thus the necessity to provide more in situ
75 deposition measurements to better constrain them.

76 [Approaches based on only some of the measurable parameters have been used to document the scavenging of](#)
77 [atmospheric particles by precipitation. One approach is to compute the washout ratio \(also called scavenging ratio](#)
78 [and hereafter referred to as WR\), which is based on the ratio of the mass or elemental concentrations of wet](#)
79 [deposition to those of aerosols measured in the atmosphere \(Chamberlain, 1960\). WR is a parameter that integrates,](#)
80 [without distinction of processes, the relative scavenging efficiency of particulate compounds and chemical](#)
81 [elements by considering their transfer from air to water. WR has been regularly used to characterize wet deposition](#)
82 [by precipitation for different types of particulate aerosols and chemical compounds found in various atmospheric](#)
83 [environments \(Jaffrezo et al., 1990; Cerqueira et al., 2010; Marticorena et al., 2017\). It can also be used to estimate](#)
84 [wet deposition fluxes given air concentrations and precipitation rates \(Duce et al., 1991; Mamun et al., 2022\).](#)
85 [Moreover, WR make it possible to study the relative importance of some of the parameters involved in the](#)
86 [mechanism of the transfer between the phases, such as rainfall rates \(González and Aristizábal, 2012\) or aerosol](#)
87 [particle size \(Jaffrezo and Colin, 1988; Cheng et al., 2021\). However, Cheng et al. \(2021\) have highlighted in their](#)
88 [literature review the scarcity of particulate element WR data due to the limited co-located measurements of](#)
89 [elements in precipitation and aerosol particles. Another approach is to calculate the scavenging coefficient, which](#)
90 [is commonly used in global chemical transport models to represent the below cloud scavenging of particles by rain](#)
91 [\(Ge et al., 2021b; Colette et al., 2017\). Theoretical studies have primarily focused on determining the particle](#)
92 [collection efficiency of raindrops as they fall, while certain numerical, laboratory, and field studies have developed](#)
93 [semi-empirical parameterizations \(Wang et al., 2014; Dépée et al., 2020; Laakso et al., 2003; Slinn, 1977\).](#)
94 [However, a gap remains between field measurements, theoretical and semi-empirical parameterizations \(Wang et](#)
95 [al., 2010, 2011\). Therefore, the determination of both WR and scavenging coefficient appears to be very useful](#)
96 [for future wet deposition studies.](#)

97 Several studies using sequential sampling have shown a decrease in concentration during the rain event, which is
98 more pronounced in the first few millimeters of rainfall (e.g., Seymour and Stout, 1983; Jaffrezo et al., 1990;
99 Aikawa and Hiraki, 2009). For example, Tanner et al., (2006) found that concentrations measured after 10 mm of
100 rainfall can be 2 to 33 times lower than concentrations measured in the first 2 mm of rainfall, depending on the
101 [studied](#) compounds ~~studied~~. Sequential rainfall sampling allows the collection of successive rainfall fractions to
102 monitor the temporal variability of wet deposition (e.g., Laquer, 1990). It is of particular interest to study the
103 dependence of wet deposition content on rainfall characteristics (intensity, droplet size and distribution), which
104 also evolve during the event (Audoux et al., 2023). In addition, the study of the chemical composition of wet
105 deposition and its evolution throughout a rain event allows determining the influences of several aerosol sources
106 (e.g., anthropogenic, [or](#) natural). The intra-event evolution of rain chemical composition has also been used to
107 discuss the relative contribution of ICS and BCS mechanisms to wet deposition (e.g., Aikawa and Hiraki, 2009;
108 Ge et al., 2021; Audoux et al., 2023). Indeed, it is generally assumed that the first increments of the rain event are
109 influenced by both mechanisms, while the last fractions could be attributed to ICS only (Aikawa and Hiraki, 2009;
110 Chatterjee et al., 2010; Germer et al., 2007; Karşı et al., 2018; Desboeufs et al., 2010), although the relative
111 proportion of ICS and BCS evolves during the event (e.g., Zou et al., 2022). Therefore, studying the evolution of
112 wet deposition composition within a rainfall event provides valuable information on the temporal variability and
113 the origin of scavenged aerosol particles, both in terms of sources of pollutant and BCS and ICS mechanisms.

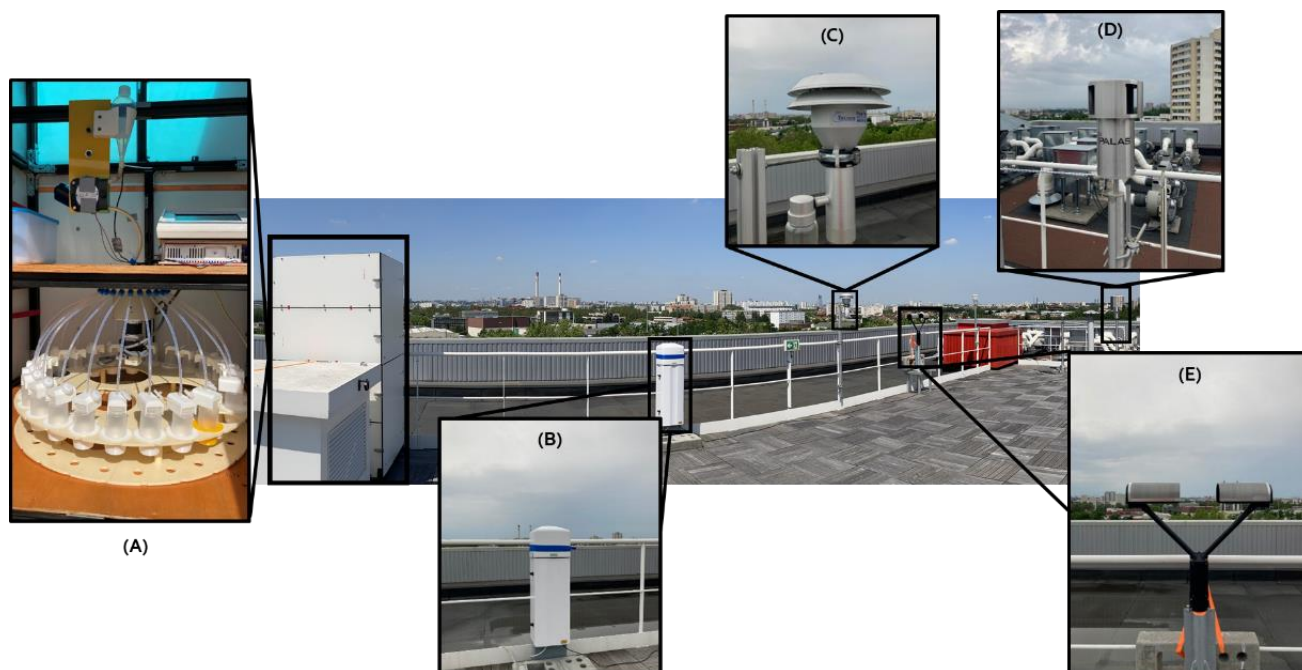
114 A dedicated sequential precipitation sampler as well as conditioning and chemical analysis protocols were
115 developed to document the intra-event variability of the dissolved and particulate chemical composition of rainfall
116 (Audoux et al., 2023). The present study is based on the analysis of sequential rainfall sampling performed in late
117 winter and spring 2022 at a study site in the Paris region, which included eight case studies with contrasting
118 meteorological conditions, atmospheric loading, and chemical composition. It has ~~three~~two objectives: (1) to
119 document the intra-event evolution of ionic and elemental composition of dissolved and particulate phase species
120 in wet deposition ~~with time and rainfall characteristics~~ for contrasted rain events, and (2) to discuss the parameters
121 influencing ~~the intra-event variability of~~ wet deposition chemistry ~~in terms of atmospheric aerosol particles~~
122 ~~sources, precipitation~~through the quantification of washout ratios and ~~meteorological properties~~scavenging
123 ~~coefficients~~ and (3) ~~to estimate~~the estimation of the relative contribution of BCS and ICS mechanisms in the wet
124 deposition.

125 **2 Material and methods**

126 **2.1 Measurement site and sampling strategy of wet deposition and aerosol particles**

127 The sampling site is located ~~on~~at the air quality station ~~site~~operated by the Interuniversity Laboratory of
128 Atmospheric Systems (LISA) ~~and located at~~, which is inside the University of Paris Est Creteil (UPEC) in the
129 south-east of the Paris agglomeration (48.79 °N-2.44 °E) (Figure 1). The study site is in close proximity to various
130 sources of pollution including nearby industries and an incinerator, highways, railway stations, and construction
131 sites. Between July 2021 and July 2022, daily rainfall depths measured using a Précis-Mécanique rain gauge model
132 3 070 A (0.2 mm precision) at the study site ranged from 0.2 to 37.6 mm. 19% of rainy days presented rainfall
133 depths lower than 0.4 mm, 12% were between 0.4 and 1 mm, 40% were between 1 and 5 mm, and 13% were
134 higher than 10 mm. The sampling strategy is to investigate case studies sampled during an intensive measurement
135 campaign during the winter and spring of 2022. During this period, the daily average PM₁₀ (PM_{2.5}) concentrations
136 were around 17.5 (11.2) µg m⁻³ with values reaching up to 57.5 (43.0) µg m⁻³. Wet deposition collection is
137 performed with a sequential sampler specifically developed at the LISA (Figure 1 A). Sampling, conditioning and
138 analysis of rain samples are described in detail in Audoux et al. (2023), and thus, it is briefly reminded here.

139 The rain is collected using a Teflon pyramid funnel with a collection surface of 1 m² in combination with a
140 sampling unit. This unit enables the automatic collection of up to 24 consecutive fractions of rain, adjustable from
141 0.05 to 2.0 mm, to study dissolved and particulate phase of the wet deposition. The sampling is conducted based
142 on volume, and as a result, it is dependent on the rainfall rate. The sequential sampler is able to correctly collect
143 rainfall fractions for low rainfall intensities, as well as for more intense rainfall recorded by the rain gauge and
144 disdrometer, in comparison with standardized measurements (Audoux et al., 2023). The materials that make up
145 the sampler have been chosen to allow analysis of the ionic and elemental composition of the dissolved and
146 particulate phase at high and low concentration levels (from several mg L⁻¹ to hundreds of ng L⁻¹). The sampling
147 bottles and materials that came in contact with the samples underwent a thorough washing protocol in clean-room
148 laboratory with ISO 7 and ISO 5 level controls.



149

150 **Figure 1: Study site. (A) Rain sequential sampler; (B) Ceilometer; (C) PM₁₀ inlet for filter sampling; (D) FIDAS; (E)**
 151 **Disdrometer**

152 A summer rain event was collected in July 2021 (R1) and a winter rain event were collected in February 2022 (R2)
 153 (Audoux et al., 2023). These case studies are completed here with 6 additional events collected in late winter and
 154 spring 2022, between March (R3, R4, R5, R6 and R7 rain events) and April (R8 rain event). For the 8 rain events
 155 studied, between 11 and 32 consecutive fractions have been sampled, the latter being collected within 10 seconds
 156 to 2 hours, depending on the rainfall rate.

157 Concomitant measurements on atmospheric aerosols and meteorological parameters during the rain sampling is
 158 important for a more in-depth understanding of wet deposition mechanisms. Therefore, PM_{2.5} and PM₁₀ aerosol
 159 mass concentration, as well as the particle size distribution (PSD) between 0.18 and 18 μm, are measured using
 160 the FIDAS (Figure 1 D), equipped with a TSP Sigma 2 inlet, with a 1 min time step. The FIDAS is an instrument
 161 used for regulatory air quality measurement of PM_{2.5} and PM₁₀ mass concentration (LCSQA, 2021). Moreover,
 162 PM₁₀ aerosol particles are sampled on polycarbonate membranes (Nuclepore®, 0.4 μm porosity) using a PM₁₀
 163 head sampling (Figure 1 C). Air sampling is done between 15 hours and 24 hours before the start of the rain and
 164 is stopped at the beginning of the latter-, within one minute after removing the cover from the sequential sampler,
 165 while the first fraction is being collected. This allows characterizing the chemical composition of the atmospheric
 166 aerosol prior to rainfall. Rainfall rate and droplet size distribution (DSD) are measured using an OTT PARSIVEL®
 167 (PARTicle Size and VELOCITY, Figure 1 E, [Supplement 1](#)) optical disdrometer with a time resolution of 30 seconds.
 168 In parallel, wind direction, wind speed as well as air temperature and relative humidity are measured using
 169 instrumentation from Campbell Scientific© and are recorded with a time step of 1 min. The cloud base height and
 170 homogeneity of atmospheric column are measured using a ceilometer (Vaisala CL31, Figure 1 B, [Supplement 2](#)).
 171 Parsivel disdrometers and ceilometers are typically used in multiple measurement networks for precipitation and
 172 cloud base height characterization (e.g., Haeffelin et al., 2005; Tapiador et al., 2010). FIDAS, ceilometer and
 173 disdrometer measurements are made continuously at the study site, while aerosols filter sampling and deposition

174 measurements are made on alert before or during rain events. This makes it necessary to regular follow-up the
175 precipitation alerts.

176 2.2 Elemental and ionic composition analysis of wet deposition samples and atmospheric aerosol membranes

177 After sampling, rain samples are quickly processed for ionic and elemental analysis, usually within a time frame
178 of 1 to 12 hours after the end of rainfall. If immediate processing is not feasible, the samples are kept in a cool and
179 dark environment at 6° C, and are processed within 24 to 48 hours. Treatment, filtration, and conditioning are done
180 in a clean-room laboratory with ISO 6 level controls, under a laminar flow hood (U15 filter) which is estimated to
181 be equivalent to ISO 3. A pH meter (METTLER TOLEDO Seven2Go) is used to measure the pH of each sequential
182 sample. Samples are then filtered through pre-cleaned Nuclepore® polycarbonate membranes with a porosity of
183 0.2 µm to separate the particulate phase from the dissolved phase. Following Audoux et al. (2023), the dissolved
184 phase is then divided into two fractions. The first fraction (10 mL aliquot) is frozen until the analysis of water-
185 soluble major inorganic cations (Na⁺, NH₄⁺, K⁺, Mg²⁺, Ca²⁺), anions (Cl⁻, NO₃⁻, PO₄³⁻, SO₄²⁻) and organic ions
186 (HCOO⁻, CH₃COO⁻, C₂H₅COO⁻, MSA, C₂O₄²⁻) by Ion Chromatography (Compact IC Flex, Metrohm®,
187 PRAMMICS Platform). The second fraction (two 15 mL aliquots) is acidified to pH = 1 with nitric acid
188 (Suprapur®) and stored at 6° C until analysis of water-soluble Al, Ba, Ca, Cr, Fe, K, Mg, Mn, Na, Ni, P, S, Si, Ti
189 and Zn by Inductively Coupled Plasma Atomic Emission Spectrometer (ICP-AES, Spectro ARCOS Ametek®).
190 The membranes are dried under laminar flow hood and conditioned for 48 h at a constant relative humidity of 45
191 – 50% and at T = 20 °C prior weighting using a precision microbalance (METTLER TOLEDO® XPR26C,
192 PRAMMICS Platform). In order to accumulate a sufficient amount of material for analysis, several rain sequential
193 samples can be filtered through the same filter. Conversely, when the particulate load is too high, rain fractions
194 can be filtered through multiple membranes. Elemental composition (Al, Ba, Ca, Cr, Fe, K, Mg, Mn, Na, Ni, P, S,
195 Si, Ti, and Zn) of the particulate phase is determined using X-ray fluorescence spectrometer (XRF, ZETIUM 4
196 kW, Malvern Panalytical, PRAMMICS Platform). The 0.4µm porosity Nuclepore® membranes are also analyzed
197 using XRF to characterize the elemental composition of the aerosol in the air prior to rainfall events. Our strategy
198 is to monitor the elemental inorganic fraction of the aerosol in order to link it to the rainfall composition. It
199 therefore allows us to characterize about 40% of the average aerosol composition in the Paris region (Airparif,
200 2021).

201 2.3 Origin of scavenged aerosol particles

202 The origin of scavenged aerosol particles can be discussed in relation with their chemical compositions
203 and the trajectory of the air masses. We calculated enrichment factors (EFs, Taylor and McLennan, 1985) in order
204 to determine the origin of elements found in the rain samples. Al is used as the reference of the Earth's crust
205 (hereafter referred to as EF_X^{crust}), and Na as reference of the sea salt (hereafter referred to as $EF_X^{sea\ salt}$). Equation
206 1 is used to calculate EF as follows:

$$207 \quad EF_X(\%) = \frac{([X]/[ref])_{rain}}{([X]/[ref])_{crust\ or\ sea\ salt}} \times 100, \quad (1)$$

208 Where $([X]/[ref])_{rain}$ correspond to the ratio between the element X and the reference (Al or Na) concentrations
209 in rainwater samples and $([X]/[ref])_{crust\ or\ sea\ salt}$ the concentrations in the continental crust or in the sea.

210 To complement local wind measurements at the study site, air mass trajectories were calculated using the
211 HYSPLIT model (<https://ready.arl.noaa.gov/HYSPLIT.php>) (Draxler and Rolph, 2012). HYSPLIT is a retro-
212 trajectory analysis used to study local to continental air mass dispersion and transport of atmospheric compounds,
213 respectively (Celle-Jeanton et al., 2009; Bertrand et al., 2008; Calvo et al., 2012), and to determine the origin of
214 air masses to identify sources of atmospheric substances, e.g., mineral dust, sea salt or anthropogenic (Vincent et
215 al., 2016; Anil et al., 2017). Here, 48 h or 120 h depending on the event, backward trajectories were computed by
216 the HYSPLIT model with GFS (0.25 °, global) from the study site (47.79 °N - 2.44 °W) at the surface (0 m a.g.l.)
217 and at the cloud base height measured by the ceilometer.

218 **2.4 Determination of washout ratios, [scavenging coefficient](#) and scavenging mechanism contributions**

219 [WR2.4.1 Washout ratios](#)

220 [The washout ratio](#) is a parameter used to quantify the relative scavenging efficiency of particulate ~~compounds and~~
221 chemical elements by rain. It is based on the principle of a transfer of the compounds from the air to the water.
222 Therefore, [below cloud](#) WR are determined from the ratio of the elemental concentration measured in the wet
223 deposition (C_{rain}) to those measured in the [aerosol filter air](#) (C_{air}) (equation 2).

$$224 \quad WR = \frac{C_{rain} (\mu g \text{ kg}^{-1})}{C_{air} (\mu g \text{ m}^{-3})} \times \rho_{air} (\text{kg m}^{-3}), \quad (2)$$

225 ~~WR make it possible to study the relative importance of some of the parameters involved in the mechanism of the~~
226 ~~transfer between the phases, such as rainfall rates or aerosol particle size . As opposed to what is done in the~~
227 ~~literature, i.e., the calculation of the WR taking into account the whole event (e.g., Here, instead to use the whole~~
228 ~~event for calculation of the WR (equation 2) as in the literature (e.g., Cheng et al., 2021), the sequential ~~collection~~~~
229 ~~makes it possible to avoid being affected by the dilution effect reported in the literature (e.g., and to use~~
230 ~~atmospheric concentrations that are more representative of the scavenged aerosol. Indeed, we calculate the WR~~
231 ~~using equation 2, but, instead of using the mean elemental concentration of the rain event, we sampling enables to~~
232 use the concentration measured in the first fraction of the rainfall, that is, the one mainly controlled by the BCS.
233 [That is more relevant regarding aerosol scavenging and determination of below-cloud WR, since this allows to](#)
234 [avoid being affected by the dilution effect reported in the literature \(e.g., Jaffrezo et al., 1990\).](#)

235 In order to discuss the relationship between aerosol and wet deposition, information is needed on both aerosol and
236 rain, which we have for R2, R3, R5 and R8. ~~In order to be able to~~ [To accurately](#) calculate the WR, [it is important](#)
237 [to consider](#) the homogeneity of the atmospheric column ~~is a parameter to be taken into account in order to justify to~~
238 [ensure](#) the representativeness of ~~the surface~~ aerosol measurements. [In our study, we observed the presence of a](#)
239 [high-altitude aerosol layer using ceilometer measurements \(Supplement S2\). The atmospheric transport of mineral](#)
240 [dust at high altitudes rendered the surface-collected aerosol sample unrepresentative of the scavenged air column.](#)
241 [As a result, we excluded the R5 study case from the WR calculation.](#) Therefore, we will ~~discuss~~ [focus our discussion](#)
242 [on](#) the WR of the element only for R2, R3, and R8.

2.4.2 Scavenging coefficient

We can determine the scavenging coefficient (Λ , s^{-1}) of elements using field measurements and based on the estimation of their washout ratios, as previously done in the literature for sulfate, nitrate and ammonium (Okita et al., 1996; Xu et al., 2019; Andronache, 2004; Yamagata et al., 2009) ~~the ICS mechanism~~. Indeed, by assuming a uniformly mixed atmospheric column below the cloud base, the average scavenging coefficient of elements can be expressed using equation (3), R and H being the rainfall rate (in $mm\ s^{-1}$) and the average cloud base height (in m) during the first fraction of rainfall, respectively.

$$\Lambda\ (s^{-1}) = WR \times \frac{R}{H} \quad (3)$$

2.4.3 In-cloud vs. below-cloud scavenging

The relative contribution of the ICS mechanism to the measured wet deposition is determined ~~using~~ by analyzing the mass concentrations of chemical species measured at the end of the rainfall (C_{ICS}), ~~a period for which there is a steady state between~~ rainfall (referred to as C_{ICS}). ~~Indeed, due to the scavenging during the initial stages of rainfall, the end of rainfall is characterized by lower PM concentration, which makes the BCS and ICS dominated by ICS, thus BCS is considered to be~~ mechanism negligible in terms of wet deposition (e.g., Aikawa and Hiraki, 2009) ~~since the rain composition can be considered representative of the concentrations of droplets in the cloud~~. Different approaches are used to determine C_{ICS} , such as measuring after a certain amount of rainfall (e.g., 5 mm; Aikawa and Hiraki, 2009; Xu et al., 2017) or selecting the lowest values during rainfall events (Karşı et al., 2018; Berberler et al., 2022). Some authors also fit an exponential decay law and use the constant value as C_{ICS} (Ge et al., 2021a), while others determine C_{ICS} using the average value obtained during periods of lower mass concentration variations (Chatterjee et al., 2010).

In our case, we selected rainfall events for which the measurements indicated an effective scavenging of the atmospheric column, with a predominant relative contribution of ICS at the end of the event. To select these events, we used the following criteria: 1) the decrease of concentrations measured in the wet deposition, reflecting the evolution of the contribution of the BCS; 2) the decrease of atmospheric concentrations measured using the FIDAS, suggesting a progressive scavenging of the air column under the cloud; and 3) constant concentrations of wet deposition at the end of the event, indicating a steady state between ICS and BCS. ~~Thus~~ From these criteria, ~~the evolution of the concentrations in the wet deposition, associated with the evolution of the atmospheric concentrations, makes it possible to discuss the~~ relative contributions of the scavenging mechanisms could be discussed for R1, R2, R4 and R8 case studies.

We determine C_{ICS} , using the VWM of the last fraction of rain, once a steady state is reached at the end of the rainfall for R1 (1.48–2.65 mm), R2 (1.02–1.33 mm for SNA and 0.89–1.33 mm for other elements), R4 (2.21 – 4.42 mm) and R8 (1.87 – 6.94 mm). The wet deposition flux due to the ICS mechanism can thus be calculated using C_{ICS} and P_{tot} , the total rainfall depth of the rainfall (equation 4) as done previously in the literature (Xu et al., 2017; Aikawa et al., 2014; Ge et al., 2021a).

277 $F_{ICS} = C_{ICS} \times P_{tot}$ (4)

278 Then, the wet deposition flux due to BCS mechanism (F_{BCS}) is determined by subtracting F_{ICS} from the total
279 (dissolved + particulate) wet deposition (F_{total}). Relative contributions of BCS (BCS_C) and ICS (ICS_C) to wet
280 deposition can be obtained using equations 5 and 6, respectively.

281 $BCS_C = \frac{F_{BCS}}{F_{total}}$ (5)

282 $ICS_C = \frac{F_{ICS}}{F_{total}}$ (6)

283 3. Results

284 3.1 Description of wet deposition case studies

285 Eight rainfalls constitute a data set illustrating various cases in terms of aerosol concentrations and compositions
286 as well as precipitation properties. The properties of the 8 rainfall events studied are listed in Table 1. The rainfall
287 events are characterized by variable rainfall depths ranging from 0.9 to 6.9 mm and mean rainfall rate from
288 0.4 mm h⁻¹ to 11.5 mm h⁻¹. Depending on the rainfall depths and rates, the sampling resolution was adapted. For
289 example, R7 was collected in 22 fractions of volumes ranging from 80 to 440 mL for a rainfall depth of 3.04 mm
290 over 30 min, while R8 was collected in 32 fractions of volumes ranging from 60 to 820 mL for a rainfall depth of
291 6.9 mm and lasted several hours. Note that for R7, the sampling setup allowed us to only collect the first 3.04 mm
292 of rain of the total event (10.3 mm). Our dataset consists of one (12.5%) event with a rainfall depth of less than
293 1 mm, one (12.5%) with a rainfall depth of more than 5 mm and the other (75%) representing rainfall depths
294 between 1 and 5 mm. [Rain events have varying cloud base heights \(from 200 m for R6 up to 2 000 m for R8\)](#)
295 [which, however, can fluctuate within the same event as it is the case for R8.](#)

296 According to the HYSPLIT 48 h back trajectory calculation, the origin of the air masses scavenged at the study
297 site remained constant during the duration of the rain events, except for R6 and R8 (Supplement S3). The air
298 masses for R1 and R2 came from the Atlantic Ocean. R3 and R4 had air masses from the Mediterranean at the
299 surface and from Spain and Portugal at the cloud base. For the other events, influenced by mineral dust intrusion
300 from North Africa, the calculation of HYSPLIT back trajectories has been performed over 120 hours with the
301 same conditions. For R5 and R6, the air masses at the surface came from the United Kingdom via the North Sea
302 and Germany, while the air masses at the cloud base came from North Africa (south of Tunisia/west of Libya) for
303 R5 and from the Mediterranean Basin and Italy for R6. In the second phase of the event R6 (after 9:00 UTC), the
304 air masses at the surface also came from the Mediterranean Basin. For R7, the air masses at the cloud base came
305 from the Mediterranean Basin and the air masses at the surface came from Libya. For R8, the beginning of the
306 event was characterized by air masses coming from the Atlantic through North Morocco and Spain at the cloud
307 base and from northern Tunisia at the surface. During the event, the origin of air masses evolved and came from
308 different places in Northern Africa (Morocco, Algeria, and Tunisia) depending on altitude. This analysis of the
309 back trajectories shows a close alignment between the origins of these large-scale air masses and the wind
310 directions measured at the surface at the instrumented site in Creteil.

311 Atmospheric aerosol mass concentrations at the beginning (average over the 30 min prior to the onset of the
312 rainfall) of R1, R2, R6 and R7 events are primarily controlled by PM_{2.5}, which represents 63–84% of PM₁₀
313 concentrations. R3 is characterized by a lower proportion of PM_{2.5}, which represents 38% of PM₁₀, while PM_{2.5}
314 measured for R4, R5 and R8 correspond to 46–53% of PM₁₀. R1 to R4 took place on days with low particle
315 concentrations, with PM₁₀ concentrations lower than of 20 µg m⁻³. During these events, rain had the effect of
316 reducing atmospheric PM₁₀ concentrations by 11–53% (Table 1). However, this illustrates the overall effect of the
317 rain event without taking into account the increases in air concentrations that may have been observed during the
318 events (e.g., R8). On the other hand, R5 to R7 occurred on days marked by high concentrations of both PM_{2.5} (33–
319 40 µg m⁻³) and PM₁₀ (47–63 µg m⁻³). The latter took place not only during a typical spring pollution episode (Favez
320 et al., 2021), but also during a mineral dust intrusion from North Africa, as shown by a multi-model dust optical
321 depth simulation provided by the WMO Barcelona Dust Regional Centre (Supplement S4S4, <https://dust.aemet.es>,
322 Basart et al., 2019). During these events, rain was less effective at reducing PM₁₀ concentrations. While R5 is
323 characterized by a decrease in the PM₁₀ concentration of the order of 17%, R6 and R7 show no variation ~~of~~ an
324 increase in the PM₁₀ concentration (Table 1). Even though R8 occurred on a day with low particle concentrations,
325 this event was also marked by the intrusion of mineral dust from northern Africa (Supplement S4S4, Table 1).

326 Total wet deposition fluxes [in our case studies](#) are ranging from 11 to 107 g m⁻²; and ~~there~~ ~~not seem to be~~ correlated
327 with rainfall depth nor rainfall rate (Table 1). ~~Although Indeed, higher~~ wet deposition fluxes are ~~higher~~ ~~observed~~
328 for [rainfall](#) events ~~characterized by (R5 and R6) associated with low rainfall depth but higher surface pre-rain~~ PM₁₀
329 ~~mass concentrations (R5, R6 and R7), they still show a factor of 4 between concentration.~~ However, events
330 characterized by a similar surface PM₁₀ mass concentration (R1, R2, R3, R4 and R8) ~~exhibit total wet deposition~~
331 [fluxes that vary over a factor 4.](#)

332 **Table 1. General information of studied rainfall events.**

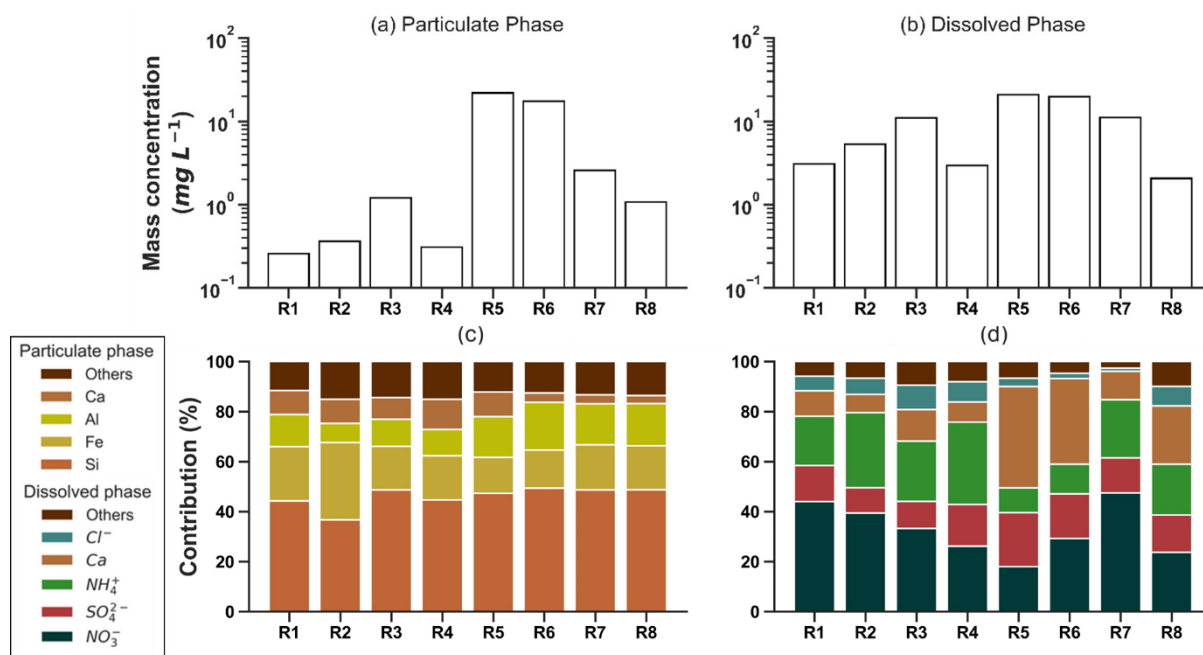
Period Date, Hour (UTC)	Rain	Number of rain fractions	Mean Rainfall depth (mm)	Mean rainfall rate (mm h ⁻¹)	Pre-rain PM ₁₀ concentration (µg m ⁻³)	PM _{2.5} /PM ₁₀ fraction (%)	After-rain PM ₁₀ concentration (µg m ⁻³)	Origin of air masses	Cloud base height (m)	Total wet deposition fluxes (g m ⁻²)	pH range
Jun.27 6:55 – 12:25	R1	21	2.65	0.48	18.7	61	12.2	West	-	11.3	5.0 – 6.0
Feb.10 17:28 – 20:55	R2	17	1.33	0.49	13.0	70	6.1	West	500 – 1 000	12.0	6.3 – 6.8
Mar.11 11:06 – 13 :19	R3	15	1.03	0.69	11.8	36	9.0	South-South West	2 000	25.7	7.8 – 7.1
Mar.11 14:16 – 17:24	R4	17	4.42	1.41	9.9	55	4.6	South	1 200 – 1 500	27.8	6.0 – 6.9
Mar.29 13:10 – 16:50	R5	11	0.90	0.40	62.6	52	52.1	North-East (surface) South (cloud base)	1 500 – 2 000	106.3	7.8 – 8.4
Mar.30 4:55 – 9:31	R6	15	1.20	0.43	44.3	82	51.7	South	200	107.1	7.2 – 8.0
Mar.30 15:32 – 16:01	R7	22	3.04	11.5	47.2	80	46.6	South	1 000	69.0	6.6 – 7.4
Apr.13 3:00 – 12 :12	R8	32	6.94	0.90	11.9	46	10.6	South	200 – 2 000	47.9	6.1 – 7.1

333 The information collected makes it possible to describe 8 case studies, illustrating contrasting situations in terms
 334 of meteorological conditions, dynamics and atmospheric ~~aerosols~~aerosol loads.

335 3.2 Classification of case studies

336 ~~Differences observed in elemental and ionic mass concentration and composition of wet deposition led us to~~
 337 ~~classify the events.~~ Volume weighted mean (VWM) mass concentrations of the particulate and dissolved phases
 338 for each rain event are represented in figure 52.

339 Regarding the particulate phase, the average ~~concentrations of major elements were found to be higher for R5 and~~
 340 ~~R6 (Al: 3 310 — 3 560 $\mu\text{g L}^{-1}$, Fe: 2 650 — 3 170 vs. $\mu\text{g L}^{-1}$, Si: 8 500 — 10 300 $\mu\text{g L}^{-1}$) by more than one order of~~
 341 ~~magnitude in comparison to R1 to R4 (Al: 28 — 130 $\mu\text{g L}^{-1}$, Fe: 54 — 210 $\mu\text{g L}^{-1}$, Si: 114 — 590 $\mu\text{g L}^{-1}$). Although~~
 342 ~~the~~ mass concentrations of ~~the major~~ elements in ~~the particulate phase of the rainfall vary within~~ exhibit high
 343 ~~variation, with values differing by~~ a factor of 85 ~~between events. The highest concentrations are observed for R5~~
 344 ~~and R6 events, with 33.9 and 34.5 mg L^{-1} , respectively. Despite these fluctuations in average mass concentrations,~~
 345 the particulate phase is ~~primarily~~predominantly composed of Si, Fe, and Al, ~~with contributing to~~ a relative
 346 ~~contribution~~proportion between 73% and 85%. In contrast, the particulate Ca content displays a more pronounced
 347 ~~variability, ranging from 73 — 85% regardless of the event. The particulate Ca content, on the other hand, was~~
 348 ~~found to vary between 3 — 3% to~~ 12% depending on the ~~specific~~ rain event.



349
 350 **Figure 52.** Volume weighted mean mass concentrations (mg L^{-1}) of (a) particulate and (b) dissolved phases. Contribution
 351 of elements in the elemental composition of particulate phase (c) and of chemical species of ionic and elemental
 352 composition of dissolved phase (d).

353 Regarding the dissolved phase, R4 and R8 are the rainfall events characterized by the lowest dissolved phase
 354 VWM concentrations (~ 2 to 3 mg L^{-1}) and the largest rainfall amounts (4.4 mm and 6.9 mm for R4 and R8,
 355 respectively). These results are consistent with the dependence of wet deposition concentrations with precipitation
 356 amount and the dilution effect documented in the literature (e.g., Jaffrezo et al., 1990). The largest concentrations

357 are of the order of 21 mg L⁻¹ and correspond to the events marked by the mineral dust intrusion from northern
 358 Africa but also the lowest precipitation amounts (0.90 mm for R5 and 1.20 mm for R6). ~~The latter are of the same~~
 359 ~~order of magnitude as values found in the literature for semi arid environments with values of the order of 20 mg L⁻¹~~
 360 ~~or for urban environments in Europe during mineral dust intrusion (11.9–20.6 mg L⁻¹;~~ marked by high contents
 361 ~~of calcium and species of crustal origin (e.g., . Dissolved Ca and SO₄²⁻ contents of the same order of magnitude~~
 362 ~~20–41% by mass are also found.~~ The rain events are not characterized by the same contents and relative
 363 proportions of acid (NO₃⁻, SO₄²⁻) or neutralizing (NH₄⁺) species depending on the rainfall. The dissolved phase is
 364 mainly composed of SO₄²⁻, NO₃⁻ and NH₄⁺ (SNA), between 58 and 85% by mass of the analyzed species for R1,
 365 R2, R3, R4, R7 and R8. In contrast, R5 and R6, and to a lesser extent R8, are composed of a non-negligible
 366 proportion of Ca in the dissolved phase (23 – 40%).

367 The variations in concentrations of not only acid species, but also neutralizing compounds, lead to different pH
 368 values in the rainfall (Table 1). The progressive scavenging of these compounds during the rainfall event also
 369 results in variations in pH (Asman et al., 1982). ~~These variations in pH can be, which is~~ observed between the
 370 different events. For instance, R1 has a lower pH (pH < 5.6) resulting from lower average concentrations of
 371 neutralizing species. Rains R2, R3, R4, R7 and R8 have higher pH values ranging from 6.2 ~~to~~ 6.8, and even basic
 372 for R5 and R6 (7.5 ~~–~~ 8.0). The basic nature of R5 and R6 rains is attributed to the higher Ca contents of mineral
 373 dusts present in these rains, which is in agreement with the influence of dust intrusion, as previously described
 374 (Ma, 2006; Oduber et al., 2020).

375 To go further in the interpretation, EFs presented in table 2 as well as origin of air masses (Table 1), are used to
 376 classify case studies into three groups: (i) R1 to R4, characterized by air masses from the west and south of France
 377 and a significant enrichment in Ca (EF > 15), Ni (EF > 10, except R4), P (EF > 30, except R1) and very high for Zn
 378 (EF > 120) and S (EF > ~~1000~~ 1000); (ii) R5 and R6, characterized by a contribution of mineral dust and EFs
 379 reflecting mineral sources signature (between 1 and 2), except for Zn (8.0 – 13) and S (119 – 136), which are still
 380 lower than the other rains; and (iii) R7 and R8, characterized by low EFs (<10) for all elements, but higher than
 381 R5 and R6 ones, except for Zn (26 – 44) and S (175 – 438).

382 **Table 2. Enrichment factors (EF^{crust}) of elements measured in the rain events relative to the upper continental crust.**
 383 **Bold values indicate significant enrichment of the element (EF^{crust} > 10).**

EF ^{crust}	Ba	Ca	Cr	Fe	K	Mg	Mn	Na	Ni	P	S	Sr	Ti	V	Zn
R1	7.9	19	5.6	2.5	3.2	1.4	3.8	4.8	17	8.1	1 281	5.4	1.7	2.6	226
R2	20	31	16	6.3	12.7	1.0	9.3	16	52	53	1 853	9.9	4.2	16	396
R3	6.6	25	5.2	2.6	5.9	1.8	5.4	13	11	33	1 060	6.3	3.0	5.0	121
R4	7.5	17	5.6	2.7	7.0	1.5	5.2	9.9	5.4	38	1 521	5.2	3.0	14	190
R5	2.6	6.6	2.3	1.4	1.2	1.0	1.5	0.37	0.9	3.8	136	2.8	1.7	3.1	13
R6	2.1	4.4	1.8	1.3	1.1	0.92	1.2	0.25	2.2	1.4	119	2.0	1.5	2.6	8.0
R7	4.2	7.1	4.1	1.8	1.6	1.1	1.9	0.53	3.7	4.1	438	2.7	1.8	3.1	44
R8	3.2	6.2	2.9	1.7	1.7	1.1	1.8	1.6	5.1	3.2	176	2.1	1.8	3.3	26

384 ~~These elements make it possible to illustrate marked differences in terms of chemical concentrations and~~
 385 ~~composition for the wet deposition events.~~ The chemical signature allows us to classify rain events into three

386 categories: R1, R2, R3 and R4 show a marked anthropogenic signature and are hereafter referred to as
387 “anthropogenic” events; R5 and R6 illustrate a distinct mineral dust signature and hereafter referred to as “mineral-
388 dust” events; when R7 and R8 correspond to mixing conditions and are hereafter referred as “~~mineral dust~~
389 ~~anthropogenic mixed~~” events. However, for a given element, the EF show that the origin is sufficiently
390 homogeneous regardless of the rain events, limiting the data analysis as a function of aerosol sources.

391 4. Discussion

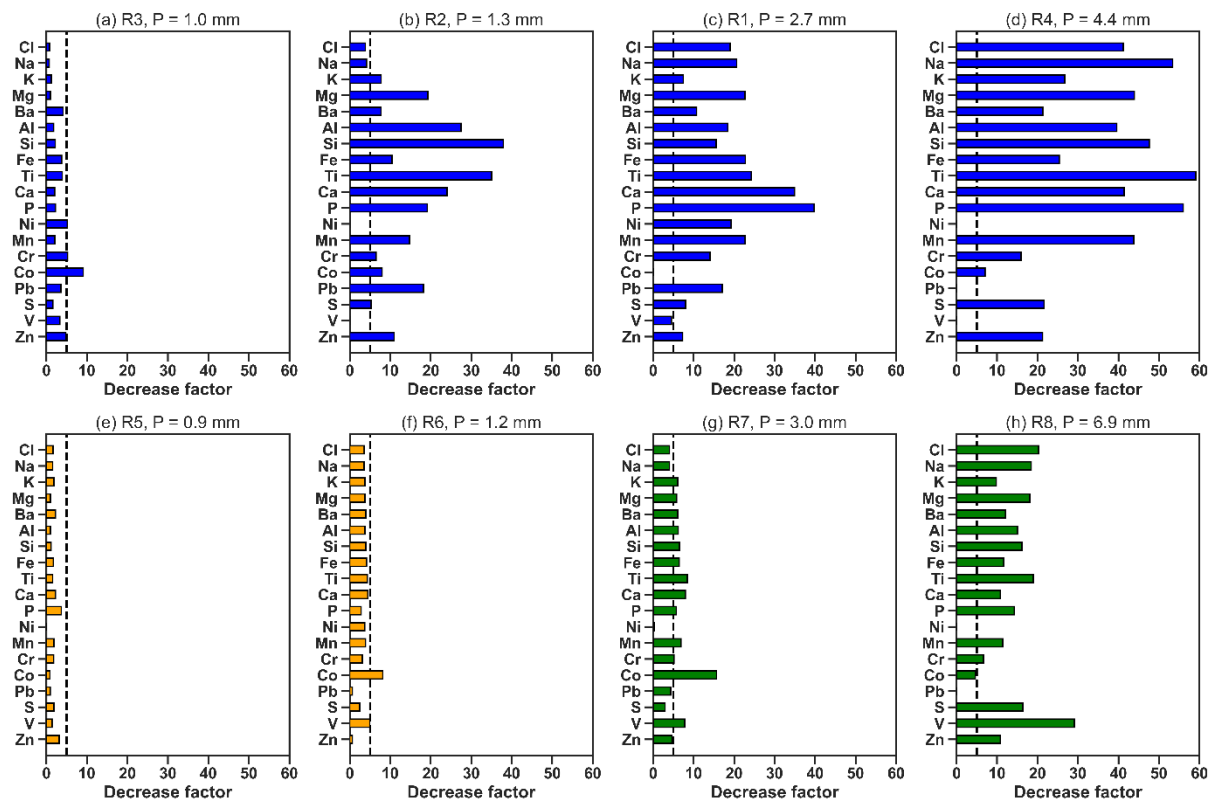
392 4.1. ~~From aerosol particles and~~ Sequential wet deposition ~~compositions to washout ratios~~ composition

393 4.1.1. Overall decrease of mass concentration

394 We firstly quantify for each event an overall decrease in mass concentrations of the particulate (up to a factor of
395 50) and dissolved (up to a factor of 35) phases, without distinction of the chemical composition (Supplement
396 S4S5). The decrease factors (DF), i.e., is computed for each rain as the ratio of the mass concentration of the first
397 fraction to the last fraction of rainfall, DF were more pronounced for “anthropogenic” than for “mineral dust”
398 rainfall, consistent with the difference in terms of rainfall amount (1.0—4.4 mm vs. 0.9—1.2 mm), and more
399 marked (R8) to 7.3 (R2) times higher for the particulate phase than for the dissolved phase, regardless of depending
400 on the event, the depth or the intensity of the rainfall. The latter appear to be. This is consistent with a more efficient
401 scavenging of coarse particles (Al, Fe and Si), predominantly in the—constituting a significant share of the
402 particulate phase mass concentration (Figure 52), compared to the secondary submicronic aerosols (SNA) that
403 make up a large proportion of the dissolved phase (Figure 52), as previously observed in the literature. However,
404 the study of the elemental DF suggests that it also varies strongly depending on the element, even when they have
405 a similar predominant phase and similar size within an event (e.g., see Supplement S5, S vs. Cl predominantly in
406 the dissolved phase [$>80\%$] and Ti vs. Cr mainly in particulate phase [$>80\%$]).

407 Figure 7 illustrates the differences in the mass concentration decrease of the elements between the first and the last
408 fraction of each rain event. Overall, we found that R3, R5 and R6 exhibit lower DF, mostly within a factor 5 for
409 R3 and R3, and within a given type of rain (“anthropogenic” Figure 3 a factor 2 for R5 (, b, c and d, “mineral dust”
410 Figure 7, Supplement S6). In contrast, DF of R1, R2, R4, R7 (except Ni) and R8 were higher, mainly greater than
411 5, depending on the element and the event. The lower DFs were observed for the events characterized by the lower
412 amount and intensity of precipitation (R3, R5 and R6), and therefore a lower efficiency to scavenge the
413 atmosphere, 3 e and f, or “mixed” Figure 3 g and h), in other words, for atmospheric content of the same order of
414 magnitude and for similar chemical composition (see Table 1 and Figure 2), the DF increases with rainfall depth
415 (Figure 3). In addition, R5 and R6 were characterized by high atmospheric aerosol concentrations and a long-range
416 transport of mineral aerosols at altitude, which also explains and low rainfall rate ($< 0.5 \text{ mm h}^{-1}$). The latter explain
417 the higher low DF, due to high mass concentrations observed at the end of throughout the event due to both the low
418 decrease of atmospheric content and the additional contribution of these dust particles within the clouds. Within a
419 given event, elemental mass concentration DF exhibits significant variability depending on the element (Figure 3),
420 even when elements share a similar predominant phase and similar size characteristics. For example, in the case
421 of R4 event, DF of Cl is two times higher than S, while they are predominantly in the last fraction dissolved phase.

422 and DF of Ti is almost 4 times higher than Cr, while they are predominantly in the particulate phase. These
 423 observations underline the importance of (a) R5 and (b) R8. The dotted line represents a 1:1 fit, while the dark and
 424 light gray envelopes represent DF within a factors 2 and 5 deviation, respectively considering individual element
 425 behaviors when assessing wet deposition dynamics.



426
 427 **Figure 3. Element decrease factor (DF) for each rain event. The dotted line marks a DF = 5. Missing bar means that the**
 428 **concentration in the first fraction and/or the last fraction of rainfall is below detection limit. Blue bars, orange bars and**
 429 **green bars correspond to “anthropogenic”, “mineral-dust” and “mixed” events, respectively.**

430 4.2.2. Intra-event evolution

431 Sequential sampling enabled the observation of various patterns of concentration evolution during rainfall events.
 432 Some events were characterized by a continuous decrease in mass concentrations throughout the rainfall,
 433 ultimately reaching a lower and constant level in the final fractions regardless of the phase nor the chemical species
 434 (R1, R7). This kind of evolution is commonly found in the literature, with a high-decreasing trend in the first 1 to
 435 3 mm, until reaching a constant level until the end of the rainfall, for both dissolved and particulate phases (e.g.,
 436 Jaffrezo et al., 1990; Kasahara et al., 1996). In contrast, although lower and constant levels were reached at the
 437 end of rainfall, other events R4, R5 and R8 exhibited punctual increases or stabilization of the concentrations of
 438 both phases during the rainfall (R4, R5 and R8), while the rest of the R2, R3 and R6 events showed only punctual
 439 increases of the dissolved phase (R2, R3 and R6).

440 As an illustration, Figure 84 shows the temporal evolution of atmospheric concentrations (PM₁₀ and PM_{2.5}) with
 441 time, the evolution of mass concentrations of dissolved and particulate phases, rainfall intensity and droplet
 442 concentrations (i.e., the number of droplets measured by the disdrometer divided by the unit of volume of the

443 collected rain fraction) during R6 and R8 events. It has been observed that atmospheric concentrations evolve
444 differently according to particle size classes (PM_{2.5} vs. PM_{2.5-10}) and rainfall phases. Generally, precipitation is
445 associated with a decrease in atmospheric concentrations during rainfall (Table 1), except for event R6 (Figure
446 ~~8-4f~~). However, an increase in concentrations of the coarse aerosol fractions (PM_{2.5-10}) is observed quite
447 systematically as rainfall intensities decrease (~~below~~ 0.5 mm h⁻¹), especially for events R2, R4, and R8 (between
448 4:00 and 5:00) as shown in Figure ~~8a4a~~.

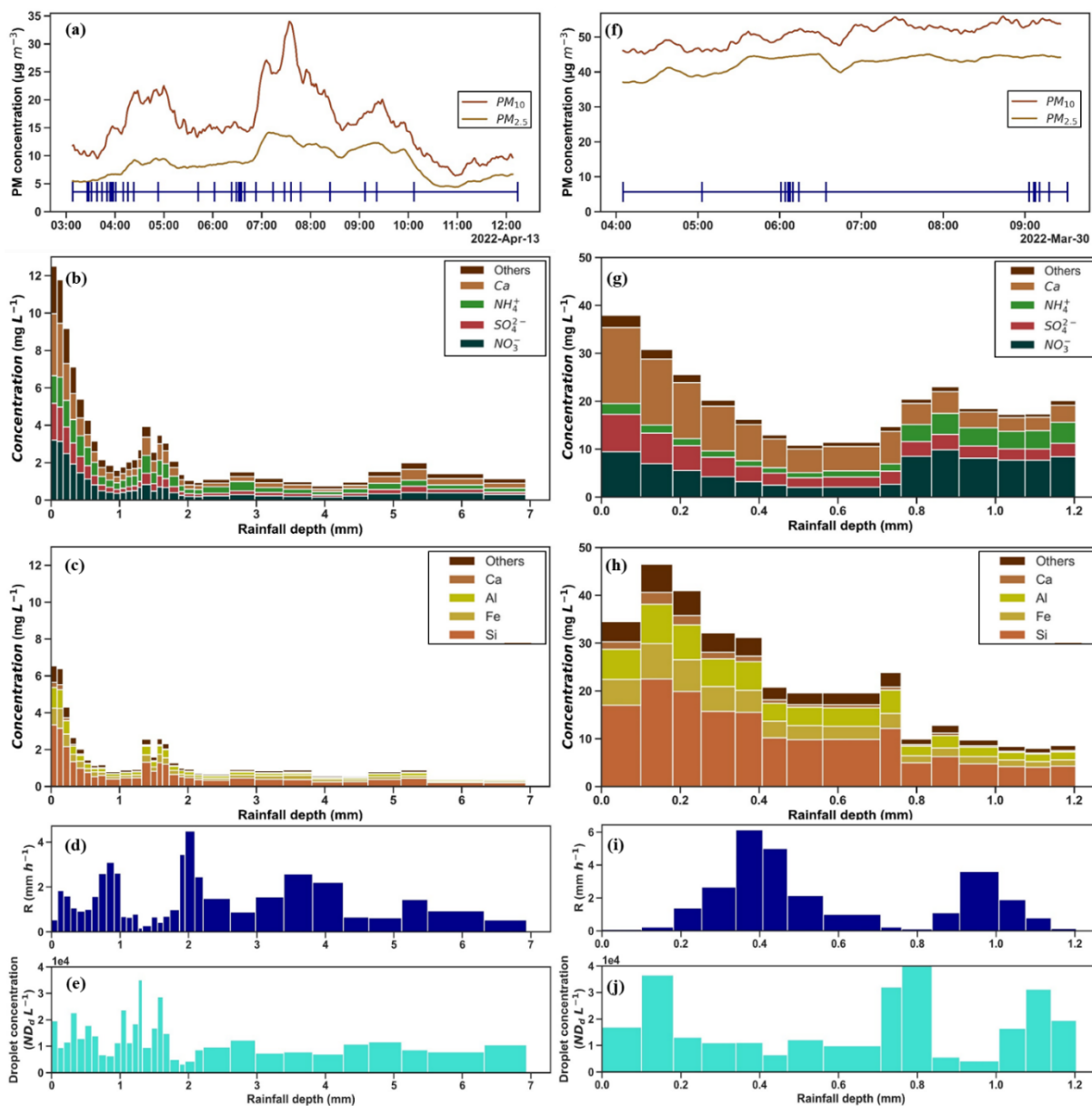
449 Increase of wet deposition concentrations during rainfall has been previously observed by some authors (e.g., Karşı
450 et al., 2018). Here, since the latter were systematically correlated with a decrease in precipitation intensity (Figure
451 ~~8-4d~~Figure 4d, i) and an increase in droplet concentration (Figure ~~8-4e~~4e, j), ~~there~~). Several possible explanations are
452 ~~considered for these observations: this could be either be~~ due to ~~1)~~ an effect of "over-concentration" of ~~the~~ falling
453 raindrops or a release of aerosols due to their evaporation (Huff and Stout, 1964; Baechmann et al., 1996a, b; Gong
454 et al., 2011); ~~or an increase in scavenging efficiency due to the reduction of droplet size distribution implying a~~
455 ~~larger effective surface of capture~~ (e.g., Jones et al., 2022), ~~or 2)~~ as well as to a local emission phenomenon (Karşı
456 et al., 2018).

457 The high temporal resolution of the sampling, and hence, the determination of the chemical composition of the
458 dissolved and particulate phases, allows identifying more accurately the cause of these concentration increases.

459 For rainfall events R4 and R8 (Figure ~~8-4a-e~~), ~~notable~~ increases in concentration during the rain are observed for
460 both the particulate and dissolved phases, ~~and are~~. ~~These increases appear to be~~ associated with higher precipitation
461 in altitudes ~~than at~~ compared to the surface ~~according to, as indicated by~~ the ceilometer measurements (~~Figure 5~~).
462 ~~A plausible explanation for these observations could be the~~ partial evaporation of raindrops as they fall ~~could~~
463 ~~thus reduce~~, leading to a reduction in their diameter and ~~concentrate them~~. ~~Assuming a subsequent increase in~~
464 ~~mass concentration. It is assumed~~ that only ~~the~~ water evaporates ~~and not in this process, while~~ the chemical species
465 contained in the raindrops ~~remain~~. Consequently, the ~~amount of~~ initial material removed by the droplets, expressed
466 in terms of their volume, ~~is~~ becomes greater (Baechmann et al., 1996b). On the contrary, if the evaporation of the
467 droplets is complete as they fall, this ~~has~~ can result in the ~~effect~~ release of ~~releasing~~ aerosols into the atmosphere,
468 thereby increasing atmospheric concentrations (Huff and Stout, 1964; Gong et al., 2011). ~~Therefore, this~~ ~~This~~
469 ~~release~~ can ~~increase then~~ affect the ~~mass~~ concentrations of ~~the following~~ subsequent raindrops ~~by capturing~~, as
470 ~~falling raindrops capture the~~ released aerosols ~~as they fall~~.

471 For R6, there is also an increase in ~~mass~~ concentrations during rainfall, but only for some species (Figure ~~8-4f-j~~).
472 NO₃⁻ and NH₄⁺ concentrations increase by a factor of 4 to 5, while dissolved Zn and Cu concentrations increase
473 by a factor of 5 to 16 (included in ~~the "others";" category in Figure 2~~). The ~~observed~~ increase in NO₃⁻ and NH₄⁺
474 ~~mass~~ concentrations in precipitation may be ~~due~~ attributed to an ~~increase in~~ additional input by local emissions.
475 ~~Indeed, During this period, between 7:00 and 9:00 a.m., low precipitation rates and a very low boundary layer~~
476 ~~height (are observed, with the cloud base height around 200 m) are observed between 7:00 and 9:00 a.m.,. This~~
477 ~~specific timeframe corresponds to a period when of significant road traffic, which is important and close in~~
478 ~~proximity~~ to the monitoring site. In addition, the NO_x concentrations measured at the LISA air quality station
479 ~~during the same time steps~~ also ~~show~~ display increases of more than a factor of 5 ~~over the same time steps~~. As,

480 [Considering that NO_x](#), Zn and Cu are tracers of automotive activity (Thorpe and Harrison, 2008; Bukowiecki et
 481 al., 2009; Pant and Harrison, 2013), this [supportsobservation provides further support for](#) the hypothesis of the
 482 influence of local emissions ([in this case](#) road traffic) on the increase in [rainfallmass](#) concentrations [of wet](#)
 483 [deposition](#) throughout the event. R6 is therefore a good case study to illustrate the combined influence of changing
 484 meteorological parameters and local sources on the evolution of deposition concentrations during a rain event.



485
 486 **Figure 84.** R8 (a-e) and R6 (f-j) case studies. Evolution of PM_{10} and $\text{PM}_{2.5}$ concentrations ($\mu\text{g m}^{-3}$; a and f) with time.
 487 The different sampling periods for each rain fraction are indicated by the intervals in blue (a and f). Evolution of
 488 dissolved mass concentration (mg L^{-1} ; b and g), particulate mass concentrations (mg L^{-1} ; c and h), rainfall intensity (R
 489 in mm h^{-1} ; d and i) and droplet concentration ($\text{ND}_d \text{ L}^{-1}$; e and j) throughout rain events.

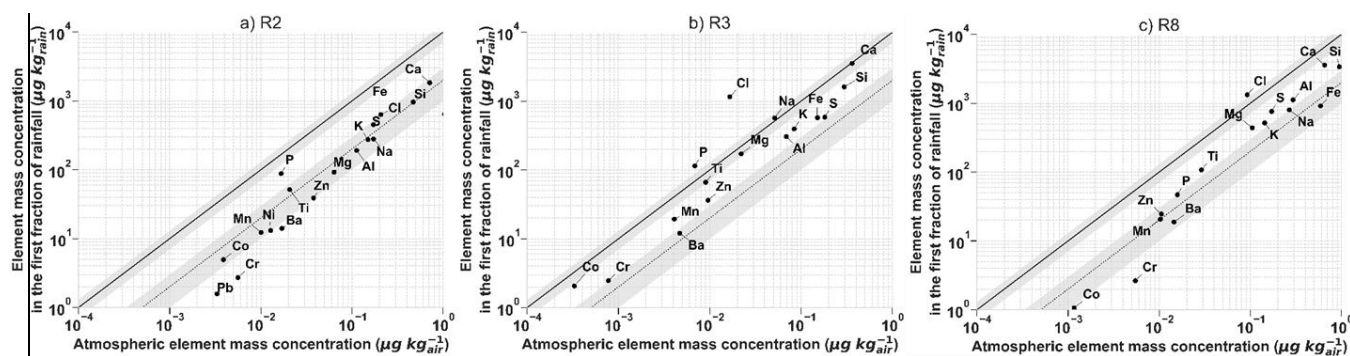
490 [By conducting a comprehensive analysis of precipitation characteristics, atmospheric dynamics, and local](#)
 491 [influences, we aimed to shed light on the underlying mechanisms responsible for the observed punctual increases](#)
 492 [in mass concentrations during our study cases. Our results highlight the importance of the droplet size distribution,](#)
 493 [its evolution as well as the presence of local sources that evolve also during the rain event. Such investigations are](#)

494 [essential to unravel the complexities of wet deposition dynamics and deepen our understanding of the intricate](#)
 495 [interactions between atmospheric particles and wet deposition processes.](#)

496 **4.2. Washout ratios and scavenging coefficient**

497 [Based on the criteria explained Sect. 2.4, we selected R1, R2, R4, The developed measurement strategy for both](#)
 498 [the chemical characterisation of aerosol and wet deposition \(see section 2.3\) enables to compare the concentrations](#)
 499 [in the air and in the first samples of rain, excluding the effect of dilution. Total mass concentrations estimated from](#)
 500 [chemical analysis of aerosol filters represent from 15 \(R3\) to 55% \(R8\) of the measured PM₁₀ mass concentration](#)
 501 [\(Table 1\), depending on the situations.](#)

502 Total mass concentrations measured in the first fraction of rainfall events (0.06 to 0.10 mm) are higher when pre-
 503 rain PM₁₀ surface concentrations are greater (Table 1). However, for R2, R3 and R8, PM₁₀ concentrations are of
 504 the same order of magnitude (11.8 – 13 µg m⁻³) while total mass concentrations in their first fraction differ by a
 505 factor 1.8 (R2: 28.1 mg L⁻¹; R3: 49.8 mg L⁻¹; R8: 38.7 mg L⁻¹). The latter is higher when the PM_{2.5}/PM₁₀ ratio is
 506 lower (Table 1). This suggests that PM_{2.5} are scavenged less effectively than coarser particles (PM_{2.5-10}). R6 and
 507 R7 events are characterized by similar pre-rain PM₁₀ surface concentrations as well as similar PM_{2.5}/PM₁₀ ratios.
 508 However, R6 event shows total mass concentrations in the first fraction 2.4 times higher than R7 (68.3 mg L⁻¹).
 509 This can be explained by the long-range transport of mineral dust in altitude. Therefore, wet deposition fluxes at
 510 the beginning of rainfall seem to be primarily correlated to PM₁₀ surface concentrations and secondly to the coarse
 511 fraction (PM_{2.5-10} / PM₁₀). This is consistent with the aerosol size dependence of scavenging mechanisms and the
 512 minimal efficiency of the BCS mechanism between 0.2 and 2 µm (e.g., Wang et al., 2010).



514 [Figure 5. Element mass concentration in the first fraction of the rainfall \(µg kg⁻¹_{rain}\) as a function of the element mass](#)
 515 [concentration in the aerosol \(µg kg⁻¹_{air}\) of \(a\) R2, \(b\) R3 and \(c\) R8. The solid lines with envelopes correspond to washout](#)
 516 [ratios of the order of 10 000 ± 3 000, while the dashed lines with envelopes correspond to washout ratios of 2 000 ± 1 000.](#)

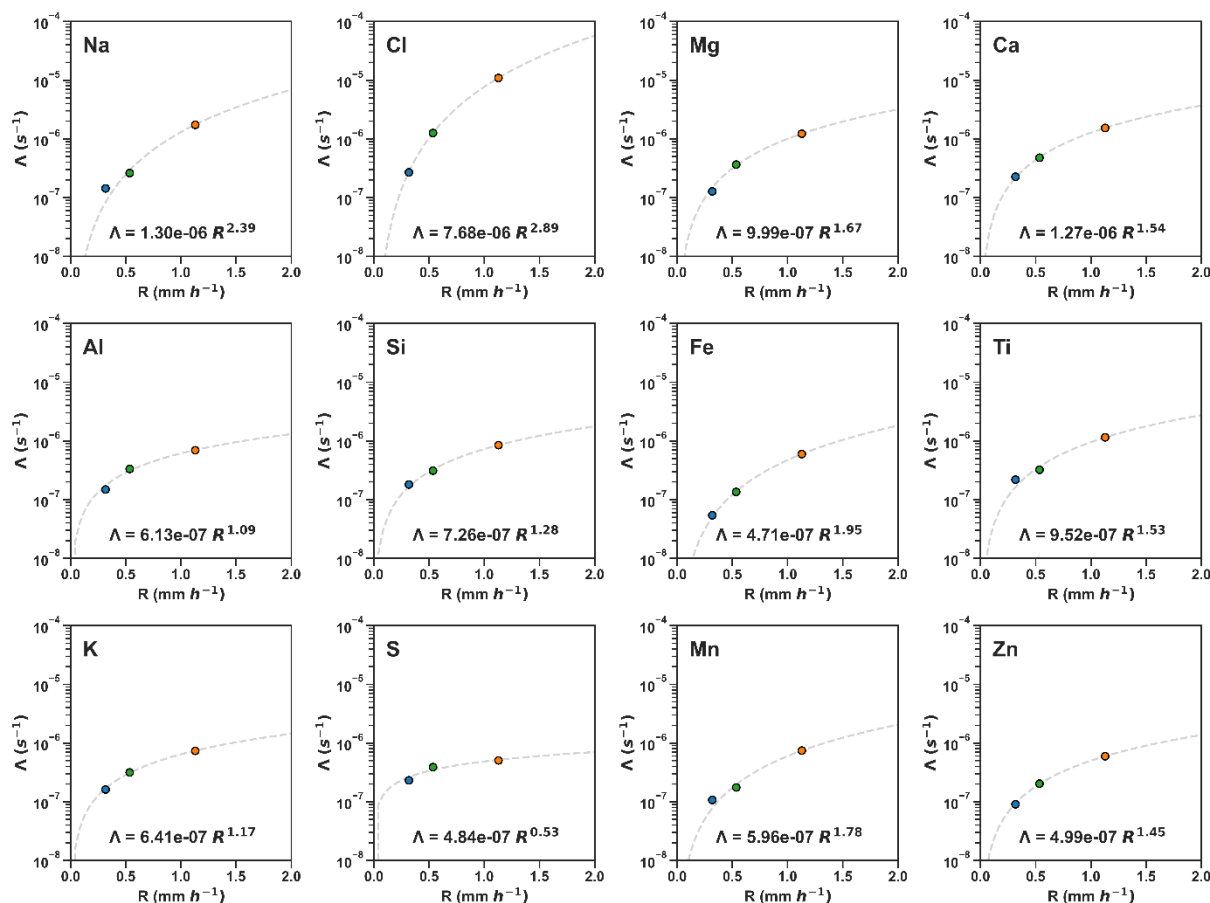
517 [Figure 5 depicts the total concentration of elements \(dissolved + particulate\) in the first rain fraction \(µg kg⁻¹_{rain}\),](#)
 518 [plotted against the total concentration of elements measured in the aerosol \(µg kg⁻¹_{air}\) for R2, R3 and R8 rain events,](#)
 519 [the only rain samplings adapted for this comparison. According to the equation 2, the ratios in these two](#)
 520 [concentrations illustrated in Figure 5 correspond to the WR for analysed species \(Supplement S6\). It appears that](#)
 521 [the scavenging efficiency is clearly depend on the element. As an example, for similar particulate mass](#)
 522 [concentrations \(0.02 µg kg⁻¹_{air}\), we found higher P concentration in the first fraction of R2 \(88 µg kg⁻¹_{rain}\) in](#)
 523 [comparison with Ba \(14 µg kg⁻¹_{rain}\).](#)

524 We found that for a given rain event, WR values can vary up to a factor of 11 to 30 from an element to another
525 (Supplement S6). WR of elements found in R2 are primarily in the $2\,000 \pm 1\,000$ envelopes, while WR of R3 are
526 systematically higher. Regarding R8 events, we observe an intermediate behavior in terms of WR values. In all
527 the cases, the values of WR are higher than the values previously estimated, in agreement with the dilution effect
528 on the WR available in the literature. Indeed, by taking into account the first fraction of the rainfall, the calculation
529 minimizes the influence of the ICS contribution as opposed to the WR values considering the entire event. The
530 difference of WR as a function of element could be due to either an additional source of elements in the rain (e.g.,
531 ICS or gas phase scavenging), a difference in BCS efficiency, e.g. due to different size distribution or
532 hygroscopicity of the element-bearing particles, or a contribution of PM with a diameter greater than $10\ \mu\text{m}$ (e.g.,
533 Jaffrezo and Colin, 1988; Cheng et al., 2021; Kasper-Giebl et al., 1999; Cheng and Zhang, 2017). Cheng et al.
534 (2021) emphasized the predominant role of particle size distribution on the WR. Indeed, the elements associated
535 with the coarse mode ($\text{PM}_{2.5-10}$) present the largest WR, except Si and Fe, while the elements that are dominant in
536 the fine particles ($\text{PM}_{2.5}$) had lower WR. Even if we have no information on the size distribution of aerosol
537 chemical composition, the EF shows that the elements associated with coarse mode by Cheng et al. (2021) are
538 from dust origin, and those associated with fine mode (e.g., S, Zn) are of anthropogenic origin, in our samples.
539 Our results are consistent with these observations: while elements linked to coarse particles, such as calcium (WR
540 ranging between 2 500 and 9 800), exhibit higher WR values compared to those associated with fine particles,
541 such as zinc (WR ranging between 1 000 and 3 800). However, as highlighted in the review of Cheng et al. (2021),
542 some elements found primarily in the coarse mode, such as Fe (WR = 3 800), exhibit similar WR value to elements
543 associated with fine particles (e.g., Zn) as illustrated in the event R3.

544 However, our study revealed a significant variation between different events for the same chemical species.
545 Interestingly, for each element, except S, this variability consistently follows a decreasing trend in WR with
546 increasing pre-rain $\text{PM}_{2.5}/\text{PM}_{10}$ fraction (Table 1). In addition, we observed an increasing trend in WR with higher
547 rainfall rates. For instance, WR of Ca increase from 2 500 to 9 800 when rainfall rate increases from 0.5 to
548 $1.2\ \text{mm h}^{-1}$. This shows that the particle size distribution is probably not the major factor acting on particle below-
549 cloud wet scavenging. These results are particularly noteworthy because they represent the first instance of WR
550 measurements unaffected by the dilution effect.

551 Scavenging coefficients (Λ) can be determined from the WR calculation using equation (3). These estimations are
552 the first available for major and trace metals. Figure 6 illustrates Λ of elements as a function of rainfall rate. Our
553 results show that Λ increases with rainfall rate according to a power law, as previously shown in the literature
554 (e.g., Xu et al., 2019; Wang et al., 2014). At a rainfall rate of $R = 1\ \text{mm h}^{-1}$, we obtained Λ values, between 0.5
555 and $1.3 \times 10^{-6}\ \text{s}^{-1}$, with the exception of chlorine. These values fall within the range ($2.6 \times 10^{-7} - 1.7 \times 10^{-6}\ \text{s}^{-1}$)
556 documented for radionuclides by Sparmacher et al. (1993). R8 events to discuss the relative contributions of ICS
557 and BCS. The ICS_c for controlled experiments with similar rainfall rate and aerosol diameters (0.98 and 2.16
558 μm). Scavenging coefficients evolution with rainfall rate that varies from one element to another, with slopes
559 ranging from 0.5 for sulphur to 2.9 for chlorine. These differences cannot be attributed solely to mass
560 concentration, particle size, or water-soluble fraction of elements. For instance, while elements associated with the
561 same aerosol types, such as Na and Cl or Al, Ti and Si, show similar behavior with rainfall rate, chlorine and

562 sulphur exhibit contrasting trends even though they are both water soluble elements. Similarly, scavenging
 563 coefficients for coarse particle (e.g., Al and Si; $1.5 - 8.5 \times 10^{-7} \text{ s}^{-1}$) are comparable to those for fine particle (Zn
 564 and S; $0.9 - 6 \times 10^{-7} \text{ s}^{-1}$). Aerosol scavenging does not depend on a single parameter, but is governed by the
 565 interaction of several parameters including the intrinsic properties of the aerosol (size, solubility) and of the
 566 precipitation (intensity, size and number of droplets). Consequently, our results underline the critical role of rainfall
 567 rates and aerosol particle properties for the determination of both WR and Λ .



568
 569 **Figure 6. Scavenging coefficient (Λ , s^{-1}) as a function of rainfall rate (R , mm h^{-1}) for studied elements.**

570 **4.3. Contribution of in-cloud and below cloud scavenging**

571 The ICS_C of chemical species analyzed in the selected rains (see 2.4) are presented in Table 3. We observe different
 572 ICS_C contributions within an event for different chemical species, as well as different We observe significant
 573 variations in ICS_C within individual events for different chemical species, as well as different ICS_C values of the
 574 same chemical species between different events.

575 **Table 3. Relative ICS_C contribution (ICS_C) for R1, R2, R4 and R8 events. Bold values indicate predominance of ICS_C .**

Chemical species	ICS_C (%)			
	R1	R2	R4	R8
SO_4^{2-}	62	48	23	58

NO₃⁻	35	55	27	57
NH₄⁺	45	40	24	65
Al	44	38	20	62
Ba	37	50	26	68
Ca	21	35	16	64
Cl	36	88	20	49
Cr	44	67	30	75
Fe	37	48	26	70
K	67	41	26	70
Mg	33	33	18	57
Mn	36	41	19	71
Na	32	85	17	53
P	24	30	17	57
Pb	82	37	18	71
Si	48	31	18	61
Sr	21	33	15	60
Ti	42	29	17	69
V	37	68	59	37
Zn	59	33	18	67
Average ± std	42 ± 15	47 ± 17	23 ± 9	62 ± 9

576 For R1, R2 and R4 anthropogenic events, the elements of crustal origin found in the coarse fraction of aerosols
577 (Al, Si, Fe, Ti, Ca, Mg, Sr) are mainly deposited via BCS mechanism. This [observation](#) is consistent with previous
578 *in situ* studies [that conducted in urban environments, which](#) have [shown](#) [reported](#) that the BCS mechanism accounts
579 for [52—a significant proportion \(ranging from 52% to 99%.\)](#) of calcium wet deposition [in urban environments](#)
580 (Ge et al., 2016; Karşı et al., 2018; Ge et al., 2021a; Berberler et al., 2022). [In contrast,](#) [The wet](#) deposition of
581 [crustal elements in mineral and anthropogenic event R8 are mainly deposited via ICS mechanism \(57—75%\).](#)

582 [With the exception of V \(37%\) and Cl \(49%\), all chemical species observed in R8 are mainly deposited through](#)
583 [ICS mechanism \(57—75%\). The characteristics of R8 suggest two possible reasons explaining ICS prevalence: 1\)](#)
584 [since the precipitation accumulation is higher, the contribution of the rainout mechanism, due to atmospheric](#)
585 [column depletion below the cloud, is also expected to be higher ; 2\) the event is characterized by a long distance](#)
586 [transport of mineral dust, which explains a more pronounced contribution of the ICS for crustal elements.](#)

587 [For anthropogenic events,](#) Mn and NH₄⁺ [was found to be](#) [is](#) mainly [deposited by](#) [attributed to](#) the BCS mechanism,
588 [between accounting for 55 and% to 87%.](#) This corresponds to a similar range of values reported for NH₄⁺ in other
589 urban environments in Austria (65%), Turkey (60 – 95%) and China (47 – 84%) (Xu et al., 2017; Karşı et al.,
590 2018; Berberler et al., 2022; Monteiro et al., 2021; Ge et al., 2021a). In the literature, [large variations are found](#)
591 [for the contribution of the BCS](#) [the BCS](#) mechanism [offor](#) sulfate and nitrate in urban environments [shows large](#)
592 [variations,](#) with [reported](#) values ranging from [50%](#) to 98% (Ge et al., 2016; Xu et al., 2017; Karşı et al., 2018; Ge

593 et al., 2021a; Monteiro et al., 2021; Berberler et al., 2022), and ~~even down to as low as~~ 16% for sulfate (Aikawa et
594 al., 2014). ~~Here, we found~~In our study, the BCS_C of sulfate and nitrate ~~ranging from~~in anthropogenic events varies
595 ~~between~~ 38 ~~to~~and 77%, depending on the events. Few chemical species show a predominance of ICS mechanism
596 in the wet deposition of anthropogenic events that could ~~be due to season explaining the difference in~~possibly be
597 ~~influenced by seasonal factors, different~~ local sources (such as oil and wood heating systems for SO₄²⁻, Zn), gas
598 scavenging contributions (with nitrate being mainly gaseous in summer and particulates in winter) (Audoux et al.,
599 2023), or long distance transport. ~~Thus, this explains~~For instance, seasonal factor and difference in local sources
600 ~~explain~~ higher ICS_C for SO₄²⁻ and Zn in R1 in comparison with R2 and R4. ~~In addition,~~ the higher ICS_C obtained
601 for Na and Cl for R2 may be ~~explained by~~linked to the origin of air masses coming from the Atlantic Ocean.
602 ~~Nevertheless~~Overall, anthropogenic events are ~~in, on~~ average ~~found to be,~~ primarily ~~controlled~~influenced by the
603 BCS mechanism ~~(, accounting for 53—% to 77%)~~-% of the wet deposition of chemical species.

604 ~~In contrast, for the mixed event R8, influenced by both local sources and long-distance transport of mineral dust,~~
605 ~~the majority of chemical species, except for V (37%) and Cl (49%), are predominantly deposited through the ICS~~
606 ~~mechanism, accounting for 57% to 75% of their wet deposition. While the long-distance transport of mineral dust~~
607 ~~may explain the pronounced contribution of the ICS mechanism for some crustal elements, it is evident that this~~
608 ~~factor alone cannot account for the prevalence of ICS for all chemical species. Certain elements observed in event~~
609 ~~R8, such as NH₄⁺, are not associated with mineral dust. Since the rainfall depth is higher in this case, the higher~~
610 ~~ICS contribution can be due to an effective scavenging of the air column below the cloud (Ge et al., 2021a)~~On the
611 ~~basis of the 4 events for which the ICS_C and BCS_C mechanisms were calculated, we cannot conclude on the~~
612 ~~influencing factors. Indeed, for the events not characterized by long range dust transport (i.e., R1, R2 and R4), no~~
613 ~~decrease in the average BCS_C with increasing rainfall depth is observed, in contrast to the findings of Ge et al.~~
614 ~~(2021). This may be due to a difference in precipitation parameters (i.e., intensity, drop size and cloud base height)~~
615 ~~and PM₁₀ concentrations (Table 1). Indeed, R1 is characterized by twice the PM₁₀ concentrations but 2 to 4 times~~
616 ~~lower precipitation depth. In addition, the cloud base height is higher for R4 compared to R2. This could be a~~
617 ~~reason why the BCS_C is higher even though the amount of precipitation is higher and the PM₁₀ concentration is~~
618 ~~lower.~~

619 ~~. Indeed, the wet deposition that occurs after the depletion of the atmospheric column below the cloud is primarily~~
620 ~~influenced by aerosol transported and scavenged within the cloud, explaining a high contribution of ICS~~
621 ~~mechanism.~~

622 ~~Several factors may contribute to these differences in the observed contribution of ICS and BCS between events.~~
623 ~~One key factor is the variation in meteorological conditions, including intensity, droplet size, and cloud base~~
624 ~~height, as well as PM₁₀ concentrations (Table 1). Numerical studies have highlighted the importance of not only~~
625 ~~cloud height but also cloud thickness in the relative contribution of BCS and ICS (Kim et al., 2021; Migliavacca~~
626 ~~et al., 2010; Wiegand et al., 2011). Therefore, cloud thickness measurements should be planned to better~~
627 ~~understand the scavenging process and its contribution to the total wet deposition~~This dependence can be explained
628 ~~by the fact that the higher the cloud height, the greater the volume of air swept by the droplets, and therefore the~~
629 ~~greater the quantity of aerosols encountered by the precipitating droplets, at equal and homogeneous concentration~~
630 ~~on the atmospheric column. For example, event R1 has higher PM₁₀ concentrations but 2 to 4 times lower rainfall~~

631 [depth compared to other anthropogenic events. In addition, R4 has a higher cloud base height compared to R2,](#)
632 [which could affect the \$BCS_C\$ despite the higher precipitation amount and lower \$PM_{10}\$ concentration. These](#)
633 [variations in meteorological conditions and atmospheric dynamic could influence \$BCS_C\$ efficiency as well as](#)
634 [aerosol content to be scavenged below the cloud, leading to the observed discrepancies in \$BCS_C\$ and \$ICS_C\$ values.](#)
635 [Consequently, the complex interactions between meteorological conditions, aerosol properties, local sources and](#)
636 [long-range transport can result in different scavenging behaviors for each event, highlighting the challenge and](#)
637 [the need of wet deposition studies.](#)

638 **5. Conclusion**

639 Measurement campaign has been done in the [south-east of the Paris ~~region~~ agglomeration](#) to monitor the evolution
640 of chemical composition of wet deposition with time during rainfall events. The collected rainfall events illustrate
641 contrasting situations in terms of meteorological conditions (rainfall depth and intensity), atmospheric dynamics
642 (cloud base height between 200 and ~~2500~~ 500 m), as well as different atmospheric PM_{10} concentrations ranging
643 from 10 to more than $60 \mu\text{g m}^{-3}$, characterized by the urban environment of the study site, but also by mineral dust
644 intrusions from the Sahara. Using additional measurements, three categories of events were identified according
645 to the origin of the aerosols found in the rain: "anthropogenic" (R1 to R4), "~~anthropogenic and~~ mineral-dust"
646 (~~R7R5~~ and ~~R8R6~~) and "~~mineral dust~~"mixed" rainfalls (~~R5R7~~ and ~~R6~~-8).

647 Our study illustrates the variability of both the mass concentrations and the chemical composition of the particulate
648 and dissolved phases. For the different rains sampled, we observe a rapid decrease in mass concentrations as the
649 rain progresses. The decrease is more pronounced for the particulate fraction (up to a factor of 50) than for the
650 dissolved fraction (up to a factor of 33), regardless of the event. [However, some phases of increasing mass](#)
651 [concentrations have been identified during certain events. We have proposed several hypotheses, such as local](#)
652 [sources, evaporation of droplets and increase of scavenging efficiency, that warrant the need to thoroughly](#)
653 [document the precipitation characteristics, atmospheric dynamics, and surface \$PM_{10}\$ and \$PM_{2.5}\$ content throughout](#)
654 [the entire rainfall event.](#)

655 [Initial chemical composition of rainfall and the chemical composition of atmospheric \$PM_{10}\$ allowed us to calculate](#)
656 [washout ratios \(WR\) describing the very beginning of the rainfall, before the dilution effect occurs when the](#)
657 [contribution of below cloud scavenging is greater. WR varied from below 2 000 for one event to up to 10 000 for](#)
658 [another, depending on the chemical species, and consistent with an increasing trend with increasing rainfall rate.](#)
659 [Scavenging coefficients were also determined based on the WR, rainfall intensity and cloud base height. We](#)
660 [obtained values in the range of \$5.4 \times 10^{-8}\$ to \$1.1 \times 10^{-5} \text{ s}^{-1}\$ for studied elements. We found a power-lawed increase of](#)
661 [the scavenging coefficient with the rainfall rate, as previously shown in the literature, indicating a greater removal](#)
662 [of particles from the atmosphere at higher rainfall intensities. However, evolutions are not directly linked to aerosol](#)
663 [size or solubility but rather to the multiple intrinsic parameters of aerosol and precipitation. The implications of](#)
664 [these results are substantial, as they emphasize the need to consider rainfall characteristics and aerosol properties](#)
665 [for accurate estimations of the scavenging process and its impact on atmospheric deposition. Such efforts will help](#)
666 [refine and develop more reliable parameterizations that can accurately represent scavenging efficiency for a wider](#)
667 [range of environmental conditions.](#)

668 We estimate the contributions of the in-cloud scavenging (ICS) and below cloud scavenging (BCS) mechanisms
669 for some rainfall events (R1, R2, R4 and R8). The results show a significant contribution of both mechanisms,
670 with a higher contribution of the BCS mechanism, between 53 and 77% in average, for rainfall events characterized
671 by a larger anthropogenic contribution and local sources (R1, R2 and R4). However, the contributions of
672 scavenging mechanisms are as variable from one chemical species to another as they are from one rainfall to
673 another, depending on their specific sources, atmospheric dynamic and meteorological conditions. The
674 anthropogenic and mineral mixed event (R8), characterized by long-distance transport of mineral dust, shows a
675 predominant contribution of the ICS mechanism. ~~This illustrates, from 57 to 75% depending on the chemical~~
676 species. It is difficult to determine a general trend based on a limited number of events, because of the complex
677 interactions between meteorological conditions, aerosol properties, local sources and long-range transport that
678 there can be contrasting situations on the same study site result in different scavenging behaviors for each event.
679 However, our findings provide new directions for future research, particularly regarding the effect of droplet size
680 distribution and the effect of cloud base height on wet deposition dynamics.

681 ~~These results highlight the importance of understanding the physical and chemical processes involved in the~~
682 ~~transfer of aerosols from the atmosphere to the precipitation in order to better assess the impact of aerosol particles~~
683 ~~pollution on the environment.~~

684 To gain a comprehensive understanding of the factors influencing scavenging mechanisms, further investigation
685 is necessary, including a larger data set covering a wider range of meteorological conditions and aerosol
686 characteristics. Such a comprehensive approach will enable a more robust analysis and to confirm and/or identify
687 the dominant factors that drive scavenging during rainfall events.

688 **Acknowledgment**

689 This work is performed in the framework of the research programs DATSHA supported by the French national
690 program LEFE (Les Enveloppes Fluides et Environnement) and Foundation Air Liquide, and was also supported
691 by LISA, UPC, UPEC, UMR CNRS 7583 via its internal project call. Some of the analyses (CI, XRF) presented
692 were performed with the instruments of the PRAMMICS platform OSU-EFLUVE UMS 3563.

693 Author contributions

694 TA: Conceptualization, Formal analysis, Investigation, Writing – original draft, Writing – review & editing,
695 Visualization. BL: Conceptualization, Investigation, Writing – review & editing, Supervision, Funding
696 acquisition, Project administration. KD: Formal analysis, Investigation, Writing – review & editing. FM:
697 Methodology, Resources. GN: Formal analysis, Resources. OL: Formal analysis. SC: Conceptualization, Formal
698 analysis, Project administration.

699 **Competing interests**

700 The authors declare that they have no known competing financial interests or personal relationships that could
701 have appeared to influence the work reported in this paper.

702 **References**

- 703 Aikawa, M. and Hiraki, T.: Washout/rainout contribution in wet deposition estimated by 0.5 mm precipitation
704 sampling/analysis, *Atmospheric Environment*, 43, 4935–4939, <https://doi.org/10.1016/j.atmosenv.2009.07.057>, 2009.
- 705 Aikawa, M., Kajino, M., Hiraki, T., and Mukai, H.: The contribution of site to washout and rainout: Precipitation chemistry
706 based on sample analysis from 0.5 mm precipitation increments and numerical simulation, *Atmospheric Environment*, 95, 165–
707 174, <https://doi.org/10.1016/j.atmosenv.2014.06.015>, 2014.
- 708 Airparif: Synthèse des connaissances sur les particules en Île-de-France, 2021.
- 709 Andronache, C.: Estimates of sulfate aerosol wet scavenging coefficient for locations in the Eastern United States, *Atmospheric
710 Environment*, 38, 795–804, <https://doi.org/10.1016/j.atmosenv.2003.10.035>, 2004.
- 711 Anil, I., Alagha, O., and Karaca, F.: Effects of transport patterns on chemical composition of sequential rain samples: trajectory
712 clustering and principal component analysis approach, *Air Quality, Atmosphere & Health*, 10, 1193–1206,
713 <https://doi.org/10.1007/s11869-017-0504-x>, 2017.
- 714 Asman, W. A. H., Jonker, P. J., Slanina, J., and Baard, J. H.: Neutralization of Acid in Precipitation and Some Results of
715 Sequential Rain Sampling, in: *Deposition of Atmospheric Pollutants: Proceedings of a Colloquium held at Oberursel/Taunus,
716 West Germany, 9–11 November 1981*, edited by: Georgii, H.-W. and Pankrath, J., Springer Netherlands, Dordrecht, 115–123,
717 https://doi.org/10.1007/978-94-009-7864-5_12, 1982.
- 718 Audoux, T., Laurent, B., Chevaillier, S., Féron, A., Pangui, E., Maisonneuve, F., Desboeufs, K., Triquet, S., Noyalet, G., Lauret,
719 O., and Huet, F.: Automatic sequential rain sampling to study atmospheric particulate and dissolved wet deposition,
720 *Atmospheric Environment*, 295, 119561, <https://doi.org/10.1016/j.atmosenv.2022.119561>, 2023.
- 721 Baechmann, K., Ebert, P., Haag, I., and Prokop, T.: The chemical content of raindrops as a function of drop radius—I. Field
722 measurements at the cloud base and below the cloud, *Atmospheric Environment*, 30, 1019–1025, [https://doi.org/10.1016/1352-
723 2310\(95\)00409-2](https://doi.org/10.1016/1352-2310(95)00409-2), 1996a.
- 724 Baechmann, K., Ebert, P., Haag, I., Prokop, T., and Steigerwald, K.: The chemical content of raindrops as a function of drop
725 radius—II. Field experimental study on the scavenging of marked aerosol particles by raindrops sampled as a function of drop
726 size, *Atmospheric Environment*, 30, 1027–1033, [https://doi.org/10.1016/1352-2310\(95\)00325-8](https://doi.org/10.1016/1352-2310(95)00325-8), 1996b.
- 727 Basart, S., Nickovic, S., Terradellas, E., Cuevas, E., García-Pando, C. P., García-Castrillo, G., Werner, E., and Benincasa, F.:
728 The WMO SDS-WAS Regional Center for Northern Africa, Middle East and Europe, E3S Web Conf., 99, 04008,
729 <https://doi.org/10.1051/e3sconf/20199904008>, 2019.
- 730 Berberler, E., Gemici, B. T., Uçun Özel, H., Demir, T., and Karakaş, D.: Source identification of water-insoluble single
731 particulate matters in rain sequences, *Atmospheric Pollution Research*, 13, 101499, <https://doi.org/10.1016/j.apr.2022.101499>,
732 2022.
- 733 Bertrand, G., Celle-Jeanton, H., Laj, P., Rangognio, J., and Chazot, G.: Rainfall chemistry: long range transport versus below
734 cloud scavenging. A two-year study at an inland station (Opme, France), *Journal of Atmospheric Chemistry*, 60, 253–271,
735 <https://doi.org/10.1007/s10874-009-9120-y>, 2008.
- 736 Bukowiecki, N., Lienemann, P., Hill, M., Figi, R., Richard, A., Furger, M., Rickers, K., Falkenberg, G., Zhao, Y., and Cliff, S.
737 S.: Real-world emission factors for antimony and other brake wear related trace elements: size-segregated values for light and
738 heavy duty vehicles, *Environmental Science & Technology*, 43, 8072–8078, 2009.
- 739 Calvo, A. I., Pont, V., Olmo, F. J., Castro, A., Alados-Arboledas, L., Vicente, A. M., Fernández-Raga, M., and Fraile, R.: Air
740 Masses and Weather Types: A Useful Tool for Characterizing Precipitation Chemistry and Wet Deposition, *Aerosol and Air
741 Quality Research*, 12, 856–878, <https://doi.org/10.4209/aaqr.2012.03.0068>, 2012.

- 742 Celle-Jeanton, H., Travi, Y., Loÿe-Pilot, M.-D., Huneau, F., and Bertrand, G.: Rainwater chemistry at a Mediterranean inland
743 station (Avignon, France): Local contribution versus long-range supply, *Atmospheric Research*, 91, 118–126,
744 <https://doi.org/10.1016/j.atmosres.2008.06.003>, 2009.
- 745 Cerqueira, M., Pio, C., Legrand, M., Puxbaum, H., Kasper-Giebl, A., Afonso, J., Preunkert, S., Gelencsér, A., and Fialho, P.:
746 Particulate carbon in precipitation at European background sites, *Journal of Aerosol Science*, 41, 51–61,
747 <https://doi.org/10.1016/j.jaerosci.2009.08.002>, 2010.
- 748 Chamberlain, A. C.: Aspects of the deposition of radioactive and other gases and particles, *Intern. J. Air Pollution*, Vol: 3,
749 1960.
- 750 Chatterjee, A., Jayaraman, A., Rao, T. N., and Raha, S.: In-cloud and below-cloud scavenging of aerosol ionic species over a
751 tropical rural atmosphere in India, *Journal of Atmospheric Chemistry*, 66, 27–40, <https://doi.org/10.1007/s10874-011-9190-5>,
752 2010.
- 753 Cheng, I. and Zhang, L.: Long-term air concentrations, wet deposition, and scavenging ratios of inorganic ions, HNO₃, and
754 SO₂ and assessment of aerosol and precipitation acidity at Canadian rural locations, *Atmos. Chem. Phys.*, 17, 4711–4730,
755 <https://doi.org/10.5194/acp-17-4711-2017>, 2017.
- 756 Cheng, I., Al Mamun, A., and Zhang, L.: A synthesis review on atmospheric wet deposition of particulate elements: scavenging
757 ratios, solubility, and flux measurements, *Environmental Reviews*, 29, 340–353, <https://doi.org/10.1139/er-2020-0118>, 2021.
- 758 Colette, A., Andersson, C., Manders, A., Mar, K., Mircea, M., Pay, M.-T., Raffort, V., Tsyro, S., Cuvelier, C., Adani, M.,
759 Bessagnet, B., Bergström, R., Briganti, G., Butler, T., Cappelletti, A., Couvidat, F., D’Isidoro, M., Doumbia, T., Fagerli, H.,
760 Granier, C., Heyes, C., Klimont, Z., Ojha, N., Otero, N., Schaap, M., Sindelarova, K., Stegehuis, A. I., Roustan, Y., Vautard,
761 R., van Meijgaard, E., Vivanco, M. G., and Wind, P.: EURODELTA-Trends, a multi-model experiment of air quality hindcast
762 in Europe over 1990–2010, *Geoscientific Model Development*, 10, 3255–3276, <https://doi.org/10.5194/gmd-10-3255-2017>,
763 2017.
- 764 Croft, B., Lohmann, U., Martin, R. V., Stier, P., Wurzler, S., Feichter, J., Hoose, C., Heikkilä, U., van Donkelaar, A., and
765 Ferrachat, S.: Influences of in-cloud aerosol scavenging parameterizations on aerosol concentrations and wet deposition in
766 ECHAM5-HAM, *Atmospheric Chemistry and Physics*, 10, 1511–1543, <https://doi.org/10.5194/acp-10-1511-2010>, 2010.
- 767 Dépée, A., Lemaitre, P., Gelain, T., Monier, M., and Flossmann, A.: Laboratory study of the collection efficiency of submicron
768 aerosol particles by cloud droplets. Part I – Influence of relative humidity, *Atmospheric Chemistry and Physics*
769 *Discussions*, 1–24, <https://doi.org/10.5194/acp-2020-831>, 2020.
- 770 Desboeufs, K., Journet, E., Rajot, J.-L., Chevaillier, S., Triquet, S., Formenti, P., and Zakou, A.: Chemistry of rain events in
771 West Africa: evidence of dust and biogenic influence in convective systems, *Atmospheric Chemistry and Physics*, 10, 9283–
772 9293, <https://doi.org/10.5194/acp-10-9283-2010>, 2010.
- 773 Draxler, R. R. and Rolph, G. D.: HYSPLIT (HYbrid Single-Particle Lagrangian Integrated Trajectory) Model access via NOAA
774 ARL READY Website, <http://ready.arl.noaa.gov/HYSPLIT.php>, 2012.
- 775 Duce, R. A., Liss, P. S., Merrill, J. T., Atlas, E. L., Buat-Menard, P., Hicks, B. B., Miller, J. M., Prospero, J. M., Arimoto, R.,
776 Church, T. M., Ellis, W., Galloway, J. N., Hansen, L., Jickells, T. D., Knap, A. H., Reinhardt, K. H., Schneider, B., Soudine,
777 A., Tokos, J. J., Tsunogai, S., Wollast, R., and Zhou, M.: The atmospheric input of trace species to the world ocean, *Global*
778 *Biogeochemical Cycles*, 5, 193–259, <https://doi.org/10.1029/91GB01778>, 1991.
- 779 Favez, O., Weber, S., Petit, J.-E., Alleman, L. Y., Albinet, A., Riffault, V., Chazeau, B., Amodeo, T., Salameh, D., Zhang, Y.,
780 Srivastava, D., Samaké, A., Aujay-Plouzeau, R., Papin, A., Bonnaire, N., Boullanger, C., Chatain, M., Chevrier, F., Detournay,
781 A., Dominik-Sègue, M., Falhun, R., Garbin, C., Ghersi, V., Grignion, G., Levigoureux, G., Pontet, S., Rangognio, J., Zhang,
782 S., Besombes, J.-L., Conil, S., Uzu, G., Savarino, J., Marchand, N., Gros, V., Marchand, C., Jaffrezo, J.-L., and Leoz-
783 Garziandia, E.: Overview of the French Operational Network for In Situ Observation of PM Chemical Composition and Sources
784 in Urban Environments (CARA Program), *Atmosphere*, 12, 207, <https://doi.org/10.3390/atmos12020207>, 2021.
- 785 Ge, B., Wang, Z., Gbaguidi, A. E., and Zhang, Q.: Source Identification of Acid Rain Arising over Northeast China: Observed
786 Evidence and Model Simulation, *Aerosol and Air Quality Research*, 16, 1366–1377,
787 <https://doi.org/10.4209/aaqr.2015.05.0294>, 2016.
- 788 Ge, B., Xu, D., Wild, O., Yao, X., Wang, J., Chen, X., Tan, Q., Pan, X., and Wang, Z.: Inter-annual variations of wet deposition
789 in Beijing from 2014–2017: implications of below-cloud scavenging of inorganic aerosols, *Atmospheric Chemistry and*
790 *Physics*, 21, 9441–9454, <https://doi.org/10.5194/acp-21-9441-2021>, 2021a.

- 791 Ge, Y., Heal, M. R., Stevenson, D. S., Wind, P., and Vieno, M.: Evaluation of global EMEP MSC-W (rv4.34) WRF (v3.9.1.1)
792 model surface concentrations and wet deposition of reactive N and S with measurements, *Geoscientific Model Development*,
793 14, 7021–7046, <https://doi.org/10.5194/gmd-14-7021-2021>, 2021b.
- 794 Germer, S., Neill, C., Krusche, A. V., Neto, S. C. G., and Elsenbeer, H.: Seasonal and within-event dynamics of rainfall and
795 throughfall chemistry in an open tropical rainforest in Rondônia, Brazil, *Biogeochemistry*, 86, 155–174,
796 <https://doi.org/10.1007/s10533-007-9152-9>, 2007.
- 797 Gong, W., Stroud, C., and Zhang, L.: Cloud Processing of Gases and Aerosols in Air Quality Modeling, *Atmosphere*, 2, 567–
798 616, <https://doi.org/10.3390/atmos2040567>, 2011.
- 799 González, C. M. and Aristizábal, B. H.: Acid rain and particulate matter dynamics in a mid-sized Andean city: The effect of
800 rain intensity on ion scavenging, *Atmospheric Environment*, 60, 164–171, <https://doi.org/10.1016/j.atmosenv.2012.05.054>,
801 2012.
- 802 Grythe, H., Kristiansen, N. I., Zwaafink, C. D. G., Eckhardt, S., Strom, J., Tunved, P., Krejci, R., and Stohl, A.: A new aerosol
803 wet removal scheme for the Lagrangian particle model FLEXPART v10, <https://doi.org/10.5194/gmd-10-1447-2017>, 2017.
- 804 Haeffelin, M., Barthès, L., Bock, O., Boitel, C., Bony, S., Bouniol, D., Chepfer, H., Chiriaco, M., Cuesta, J., Delanoë, J.,
805 Drobinski, P., Dufresne, J.-L., Flamant, C., Grall, M., Hodzic, A., Hourdin, F., Lapouge, F., Lemaître, Y., Mathieu, A., Morille,
806 Y., Naud, C., Noël, V., O'Hirok, W., Pelon, J., Pietras, C., Protat, A., Romand, B., Scialom, G., and Vautard, R.: SIRTa, a
807 ground-based atmospheric observatory for cloud and aerosol research, *Annales Geophysicae*, 23, 253–275,
808 <https://doi.org/10.5194/angeo-23-253-2005>, 2005.
- 809 Huff, F. A. and Stout, G. E.: Distribution of Radioactive Rainout in Convective Rainfall, *Journal of Applied Meteorology*
810 (1962-1982), 3, 707–717, 1964.
- 811 Jaffrezo, J.-L. and Colin, J.-L.: Rain-aerosol coupling in urban area: Scavenging ratio measurement and identification of some
812 transfer processes, *Atmospheric Environment* (1967), 22, 929–935, [https://doi.org/10.1016/0004-6981\(88\)90270-3](https://doi.org/10.1016/0004-6981(88)90270-3), 1988.
- 813 Jaffrezo, J.-L., Colin, J.-L., and Gros, J.-M.: Some physical factors influencing scavenging ratios, *Atmospheric Environment*.
814 Part A. General Topics, 24, 3073–3083, [https://doi.org/10.1016/0960-1686\(90\)90486-7](https://doi.org/10.1016/0960-1686(90)90486-7), 1990.
- 815 Jones, A. C., Hill, A., Hemmings, J., Lemaître, P., Quérel, A., Ryder, C. L., and Woodward, S.: Below-cloud scavenging of
816 aerosol by rain: a review of numerical modelling approaches and sensitivity simulations with mineral dust in the Met Office's
817 Unified Model, *Atmospheric Chemistry and Physics*, 22, 11381–11407, <https://doi.org/10.5194/acp-22-11381-2022>, 2022.
- 818 Karşı, M. B. B., Yenisoy-Karakaş, S., and Karakaş, D.: Investigation of washout and rainout processes in sequential rain
819 samples, *Atmospheric Environment*, 190, 53–64, <https://doi.org/10.1016/j.atmosenv.2018.07.018>, 2018.
- 820 Kasahara, M., Ogiwara, H., and Yamamoto, K.: Soluble and insoluble components of air pollutants scavenged by rain water,
821 *Nuclear Instruments and Methods in Physics Research Section B: Beam Interactions with Materials and Atoms*, 118, 400–402,
822 [https://doi.org/10.1016/0168-583X\(95\)01087-4](https://doi.org/10.1016/0168-583X(95)01087-4), 1996.
- 823 Kasper-Giebl, A., Kalina, M. F., and Puxbaum, H.: Scavenging ratios for sulfate, ammonium and nitrate determined at Mt.
824 Sonnblick (3106m a.s.l.), *Atmospheric Environment*, 33, 895–906, [https://doi.org/10.1016/S1352-2310\(98\)00279-9](https://doi.org/10.1016/S1352-2310(98)00279-9), 1999.
- 825 Kim, K. D., Lee, S., Kim, J.-J., Lee, S.-H., Lee, D., Lee, J.-B., Choi, J.-Y., and Kim, M. J.: Effect of Wet Deposition on
826 Secondary Inorganic Aerosols Using an Urban-Scale Air Quality Model, *Atmosphere*, 12, 168,
827 <https://doi.org/10.3390/atmos12020168>, 2021.
- 828 Laakso, L., Grönholm, T., Rannik, Ü., Kosmale, M., Fiedler, V., Vehkamäki, H., and Kulmala, M.: Ultrafine particle
829 scavenging coefficients calculated from 6 years field measurements, *Atmospheric Environment*, 37, 3605–3613,
830 [https://doi.org/10.1016/S1352-2310\(03\)00326-1](https://doi.org/10.1016/S1352-2310(03)00326-1), 2003.
- 831 Laquer, F. C.: Sequential precipitation samplers: A literature review, *Atmospheric Environment. Part A. General Topics*, 24,
832 2289–2297, [https://doi.org/10.1016/0960-1686\(90\)90322-E](https://doi.org/10.1016/0960-1686(90)90322-E), 1990.
- 833 LCSQA: Conformité technique des appareils de mesure, Laboratoire Central de Surveillance de la Qualité de l'Air, 2021.
- 834 Lim, B., Jickells, T. D., and Davies, T. D.: Sequential sampling of particles, major ions and total trace metals in wet deposition,
835 *Atmospheric Environment. Part A. General Topics*, 25, 745–762, [https://doi.org/10.1016/0960-1686\(91\)90073-G](https://doi.org/10.1016/0960-1686(91)90073-G), 1991.

- 836 Ma, C.-J.: Chemical composition of a yellowish rainfall by the application of PIXE and micro-PIXE technique, *Nuclear*
837 *Instruments and Methods in Physics Research Section B: Beam Interactions with Materials and Atoms*, 251, 501–506,
838 <https://doi.org/10.1016/j.nimb.2006.07.025>, 2006.
- 839 Mamun, A. A., Cheng, I., Zhang, L., Celo, V., Dabek-Zlotorzynska, E., and Charland, J.-P.: Estimation of Atmospheric Dry
840 and Wet Deposition of Particulate Elements at Four Monitoring Sites in the Canadian Athabasca Oil Sands Region, *Journal of*
841 *Geophysical Research: Atmospheres*, 127, e2021JD035787, <https://doi.org/10.1029/2021JD035787>, 2022.
- 842 Marticorena, B., Chatenet, B., Rajot, J. L., Bergametti, G., Deroubaix, A., Vincent, J., Kouoi, A., Schmechtig, C., Coulibaly,
843 M., Diallo, A., Koné, I., Maman, A., NDiaye, T., and Zakou, A.: Mineral dust over west and central Sahel: Seasonal patterns
844 of dry and wet deposition fluxes from a pluriannual sampling (2006–2012), *Journal of Geophysical Research: Atmospheres*,
845 122, 1338–1364, <https://doi.org/10.1002/2016JD025995>, 2017.
- 846 Migliavacca, D. M., Teixeira, E. C., Raya Rodriguez, M. T., Wiegand, F., and Pereira, F. N.: Analysis of the sulfate aerosol
847 scavenging processes in the metropolitan area of Porto Alegre (MAPA), RS, Brazil, *Atmospheric Pollution Research*, 1, 82–
848 93, <https://doi.org/10.5094/APR.2010.011>, 2010.
- 849 Monteiro, L. R., Terzer-Wasmuth, S., Matiatos, I., Douence, C., and Wassenaar, L. I.: Distinguishing in-cloud and below-
850 cloud short and distal N-sources from high-temporal resolution seasonal nitrate and ammonium deposition in Vienna, Austria,
851 *Atmospheric Environment*, 266, 118740, <https://doi.org/10.1016/j.atmosenv.2021.118740>, 2021.
- 852 Oduber, F., Calvo, A. I., Castro, A., Blanco-Alegre, C., Alves, C., Barata, J., Nunes, T., Lucarelli, F., Nava, S., Calzolari, G.,
853 Cerqueira, M., Martín-Villacorta, J., Esteves, V., and Fraile, R.: Chemical composition of rainwater under two events of aerosol
854 transport: A Saharan dust outbreak and wildfires, *Science of The Total Environment*, 734, 139202,
855 <https://doi.org/10.1016/j.scitotenv.2020.139202>, 2020.
- 856 Okita, T., Hara, H., and Fukuzaki, N.: Measurements of atmospheric SO₂ and SO₄²⁻, and determination of the wet scavenging
857 coefficient of sulfate aerosols for the winter monsoon season over the sea of Japan, *Atmospheric Environment*, 30, 3733–3739,
858 [https://doi.org/10.1016/1352-2310\(96\)00090-8](https://doi.org/10.1016/1352-2310(96)00090-8), 1996.
- 859 Pant, P. and Harrison, R. M.: Estimation of the contribution of road traffic emissions to particulate matter concentrations from
860 field measurements: A review, *Atmospheric Environment*, 77, 78–97, <https://doi.org/10.1016/j.atmosenv.2013.04.028>, 2013.
- 861 Ryu, Y.-H. and Min, S.-K.: Improving Wet and Dry Deposition of Aerosols in WRF-Chem: Updates to Below-Cloud
862 Scavenging and Coarse-Particle Dry Deposition, *Journal of Advances in Modeling Earth Systems*, 14, e2021MS002792,
863 <https://doi.org/10.1029/2021MS002792>, 2022.
- 864 Seinfeld, J. H. and Pandis, S. N.: *Atmospheric Chemistry and Physics: From Air Pollution to Climate Change*, John Wiley &
865 Sons, 1146 pp., 2016.
- 866 Seymour, M. D. and Stout, T.: Observations on the chemical composition of rain using short sampling times during a single
867 event, *Atmospheric Environment* (1967), 17, 1483–1487, [https://doi.org/10.1016/0004-6981\(83\)90301-3](https://doi.org/10.1016/0004-6981(83)90301-3), 1983.
- 868 Slinn, W. G. N.: Some approximations for the wet and dry removal of particles and gases from the atmosphere, *Water, Air,*
869 *and Soil Pollution*, 7, <https://doi.org/10.1007/BF00285550>, 1977.
- 870 Sparmacher, H., Fülber, K., and Bonka, H.: Below-cloud scavenging of aerosol particles: Particle-bound radionuclides—
871 Experimental, *Atmospheric Environment. Part A. General Topics*, 27, 605–618, [https://doi.org/10.1016/0960-1686\(93\)90218-](https://doi.org/10.1016/0960-1686(93)90218-N)
872 N, 1993.
- 873 Tanner, P. A., Tam, C. W. F., Tanner, P. A., and Tam, C. W. F.: In-Cloud Concentrations and Below-Cloud Scavenging
874 Processes in Hong Kong, China, *Environ. Chem.*, 3, 142–148, <https://doi.org/10.1071/EN05084>, 2006.
- 875 Tapiador, F. J., Checa, R., and de Castro, M.: An experiment to measure the spatial variability of rain drop size distribution
876 using sixteen laser disdrometers, *Geophysical Research Letters*, 37, <https://doi.org/10.1029/2010GL044120>, 2010.
- 877 Taylor, S. R. and McLennan, S. M.: *The continental crust: Its composition and evolution*, 1985.
- 878 Thorpe, A. and Harrison, R. M.: Sources and properties of non-exhaust particulate matter from road traffic: A review, *Science*
879 *of The Total Environment*, 400, 270–282, <https://doi.org/10.1016/j.scitotenv.2008.06.007>, 2008.
- 880 Vincent, J., Laurent, B., Losno, R., Bon Nguyen, E., Rouillet, P., Sauvage, S., Chevaillier, S., Coddeville, P., Ouboulmane, N.,
881 di Sarra, A. G., Tovar-Sánchez, A., Sferlazzo, D., Massanet, A., Triquet, S., Morales Baquero, R., Fournier, M., Coursier, C.,

882 Desboeufs, K., Dulac, F., and Bergametti, G.: Variability of mineral dust deposition in the western Mediterranean basin and
883 south-east of France, *Atmospheric Chemistry and Physics*, 16, 8749–8766, <https://doi.org/10.5194/acp-16-8749-2016>, 2016.

884 Wang, X., Zhang, L., and Moran, M. D.: Uncertainty assessment of current size-resolved parameterizations for below-cloud
885 particle scavenging by rain, *Atmos. Chem. Phys.*, 10, 5685–5705, <https://doi.org/10.5194/acp-10-5685-2010>, 2010.

886 Wang, X., Zhang, L., and Moran, M. D.: On the discrepancies between theoretical and measured below-cloud particle
887 scavenging coefficients for rain – a numerical investigation using a detailed one-dimensional cloud microphysics model,
888 *Atmospheric Chemistry and Physics*, 11, 11859–11866, <https://doi.org/10.5194/acp-11-11859-2011>, 2011.

889 Wang, X., Zhang, L., and Moran, M. D.: Development of a new semi-empirical parameterization for below-cloud scavenging
890 of size-resolved aerosol particles by both rain and snow, *Geosci. Model Dev.*, 7, 799–819, [https://doi.org/10.5194/gmd-7-799-](https://doi.org/10.5194/gmd-7-799-2014)
891 2014, 2014.

892 Wiegand, F., Pereira, F. N., and Teixeira, E. C.: Study on wet scavenging of atmospheric pollutants in south Brazil,
893 *Atmospheric Environment*, 45, 4770–4776, <https://doi.org/10.1016/j.atmosenv.2010.02.020>, 2011.

894 Xu, D., Ge, B., Wang, Z., Sun, Y., Chen, Y., Ji, D., Yang, T., Ma, Z., Cheng, N., Hao, J., and Yao, X.: Below-cloud wet
895 scavenging of soluble inorganic ions by rain in Beijing during the summer of 2014, *Environmental Pollution*, 230, 963–973,
896 <https://doi.org/10.1016/j.envpol.2017.07.033>, 2017.

897 Xu, D., Ge, B., Chen, X., Sun, Y., Cheng, N., Li, M., Pan, X., Ma, Z., Pan, Y., and Wang, Z.: Multi-method determination of
898 the below-cloud wet scavenging coefficients of aerosols in Beijing, China, *Atmospheric Chemistry and Physics*, 19, 15569–
899 15581, <https://doi.org/10.5194/acp-19-15569-2019>, 2019.

900 Yamagata, S., Kobayashi, D., Ohta, S., Murao, N., Shiobara, M., Wada, M., Yabuki, M., Konishi, H., and Yamanouchi, T.:
901 Properties of aerosols and their wet deposition in the arctic spring during ASTAR2004 at Ny-Alesund, Svalbard, *Atmospheric
902 Chemistry and Physics*, 10, 2009.

903 Yang, Q., Easter, R. C., Campuzano-Jost, P., Jimenez, J. L., Fast, J. D., Ghan, S. J., Wang, H., Berg, L. K., Barth, M. C., Liu,
904 Y., Shrivastava, M. B., Singh, B., Morrison, H., Fan, J., Ziegler, C. L., Bela, M., Apel, E., Diskin, G. S., Mikoviny, T., and
905 Wisthaler, A.: Aerosol transport and wet scavenging in deep convective clouds: A case study and model evaluation using a
906 multiple passive tracer analysis approach, *Journal of Geophysical Research: Atmospheres*, 120, 8448–8468,
907 <https://doi.org/10.1002/2015JD023647>, 2015.

908 Zou, C., Yang, X., Zhang, Y., and Huang, H.: Characteristics and distribution of inorganic ions in segmented precipitation and
909 contribution of below-cloud/in-cloud scavenging in Nanchang, *Air Qual Atmos Health*, 15, 903–916,
910 <https://doi.org/10.1007/s11869-022-01166-3>, 2022.

911